# Radiative Transfer in Entry Flows

## 10th International Planetary Probe Workshop, EDL Short Course
## San José, California, 15–21 June 2013

M. Lino da Silva[1] and Lionel Marraffa[2]

[1]: Instituto de Plasmas e Fusão Nuclear
Instituto Superior Técnico, Lisboa, Portugal
[2]: ESA–ESTEC, Aerothermodynamics Section
Noordwijk, The Netherlands

15 June 2013

# Introduction

- Radiative heating can be a major design driver for large or high-speed ($\geq 10 km/s$) entry vehicles
- For lower entry speeds, radiative heating may mandate additional thermal protections (e.g. base heating for Martian entries)
- Convective heating mostly depends on ground species, radiative heating depends on excited species. Larger uncertainties
- Accounting for an additional spectral dimension with grids with over $10^6$ points. Very computationally intensive CFRD simulations.

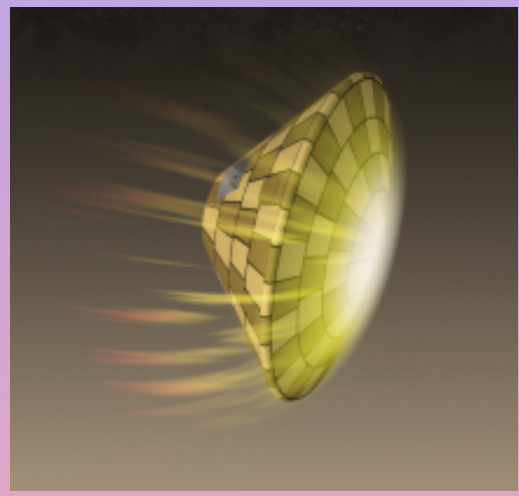

# Main Drivers

- Do we need to take radiation into account?
- Optically thin or thick?
- Coupling between flow and radiation?
- Equilibrium or non-equilibrium radiation?
- Selection of an appropriate radiative database
- Other issues (precursor, photo-chemistry, photo-ionisation processes)

# Aerothermodynamics of Entry Vehicles

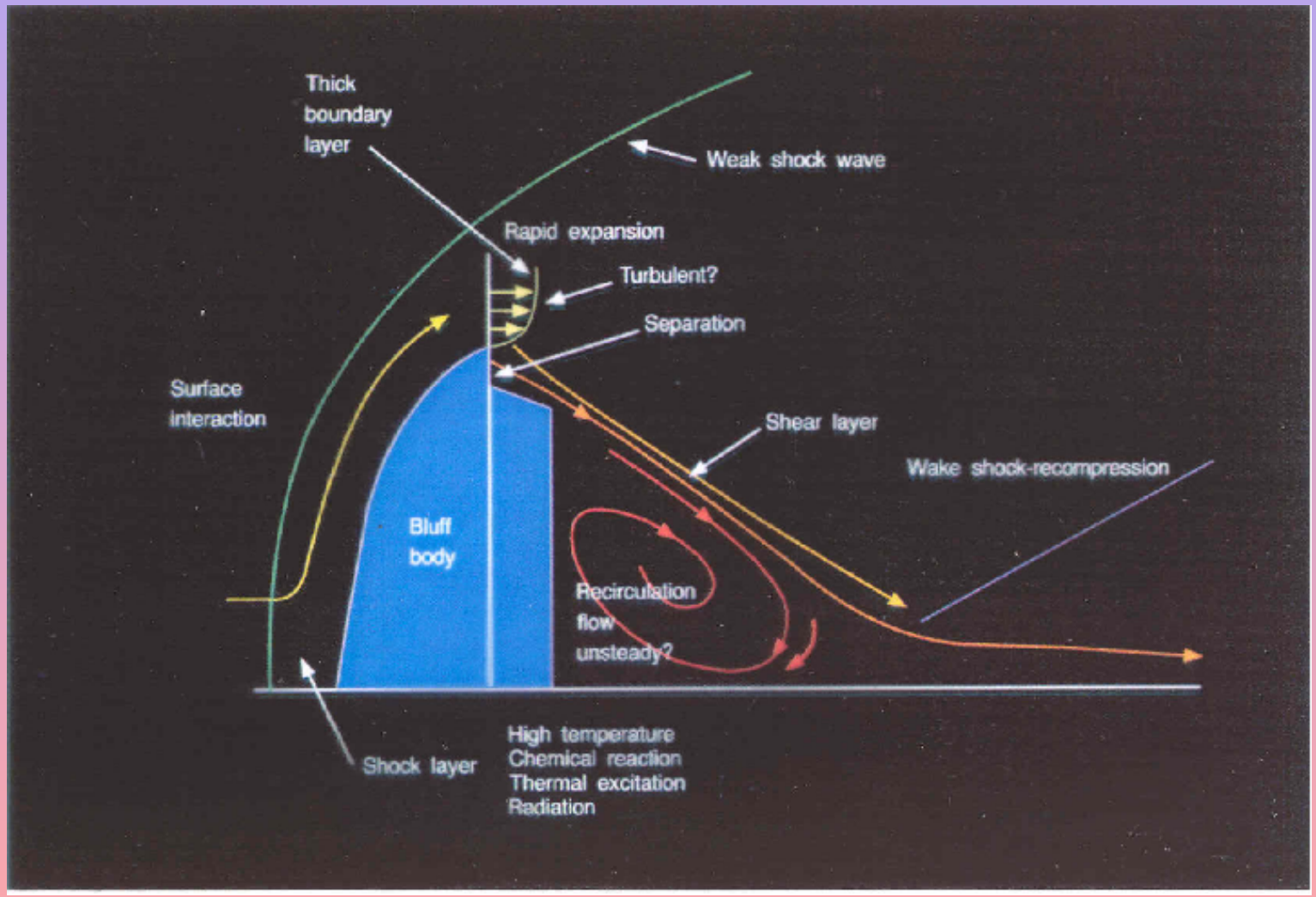

# Aerothermodynamics of Entry Vehicles

*Fluid*
- Thermal non-equilibrium
- Chemical non-equilibrium
- Ionisation

*Heat shield*
- Pyrolysis
- Charring
- Mechanical erosion

*Surface*
- Recombination
- Re-radiation
- Surface reactions

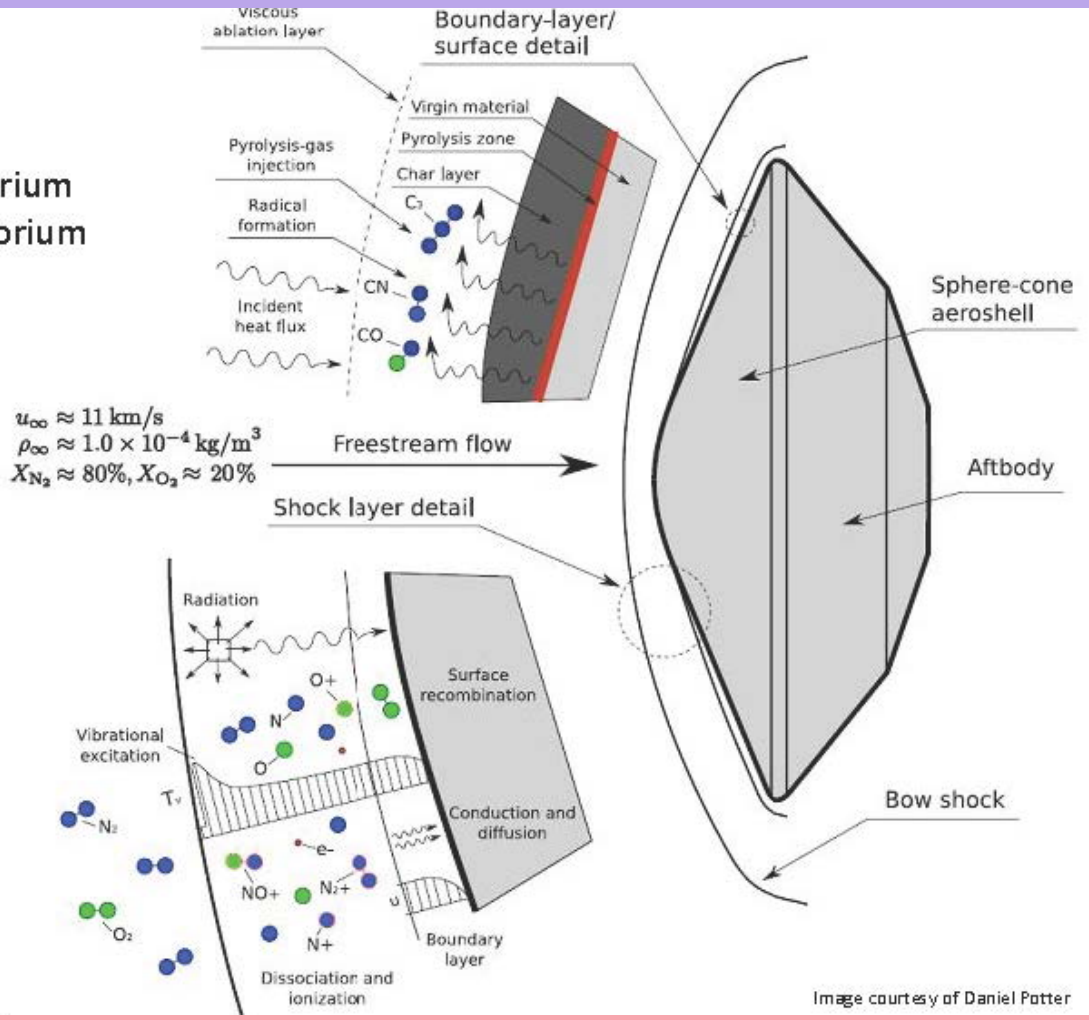

# Engineering Correlations for Radiation

- Engineering Correlations useful when exploring different EDL scenarios
- Exploratory paameters: Spacecraft sizing, atmospheric profiles and composition, entry path and angle, aerodymamic coefficients, etc...
- Correlations then complemented with detailed CFRD calculations for pre-selected Flight pathss, at specific representative entry points ($\sim$5)

# Blackbody radiation limit

spectral emissivity of a gas has a theoretical limit given by Planck's law

$$B_\nu(T) = \frac{2h\nu^3}{c^2}\left[exp\left(\frac{h\nu}{k_B T}\right) - 1\right]^{-1}$$

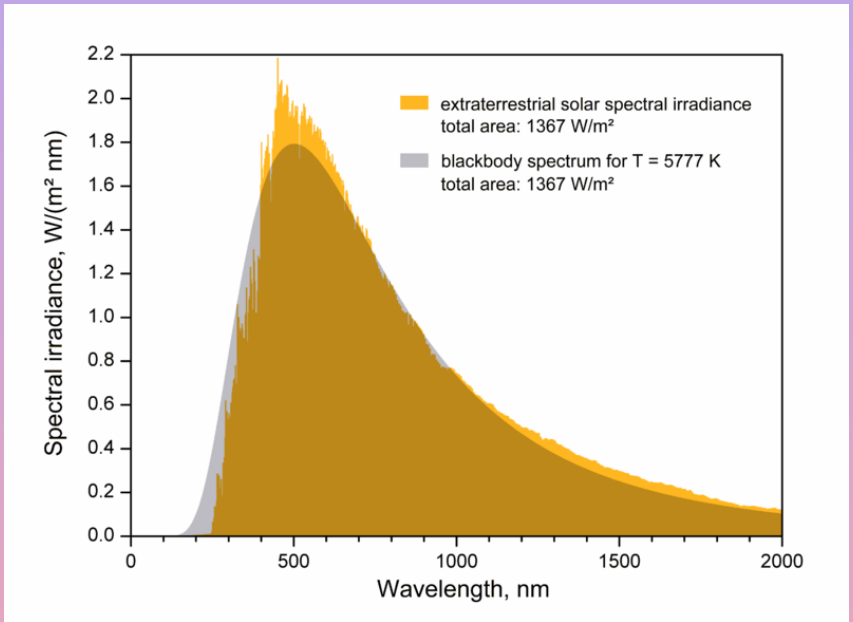


The Sun's emissivity is close to a blackbody

The spectral integration yields the Stefan–Boltzmann Law:

$$\int_\nu B_\nu(T) = \sigma T^4$$

Engineering correlations are based on this upper theoretical limit for the emitted radiation

# Stagnation Streamline flux dependence on cone radius

- **Convective fluxes**
  Sutton and Graves, Fay and Riddel correlations:
  $q^w_{conv} = f\left[\sqrt{\left(\frac{du}{dx}\right)_s}\right]$
  from Newtonian theory: $\left[\left(\frac{du}{dx}\right)_s\right] = \frac{1}{R}\sqrt{\frac{2p-p_\infty}{\rho}}$
  $q^w_{conv} \propto \frac{1}{\sqrt{R}}$
- **Radiative Fluxes**
  Optically Thin shock layer: $q^w_{rad} = \left(\frac{E\delta}{2}\right)^a$ with $\delta \backsimeq \frac{R}{\rho_s/\rho_\infty}$
  $q^w_{rad} \propto R$
  Requirements for minimizing convective and radiative heat fluxes are mutually exclusive

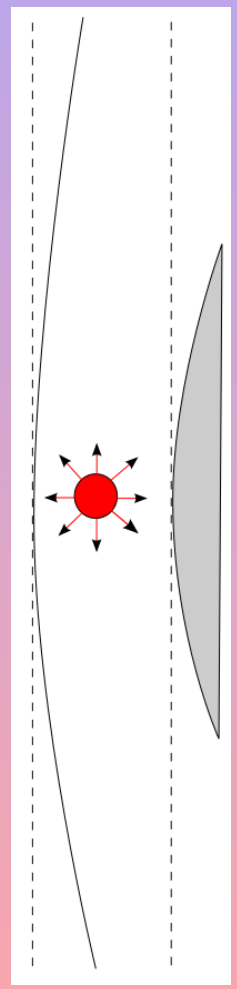

[a] E: radiated power, half goes upstream, half to the wall. $\delta$ is the shock standoff. $s$: shock

# Stagnation Streamline flux dependence on entry speed

- **Convective fluxes**

  $q^w_{conv} \approx 1/2 \rho_\infty u^3_\infty \mathrm{St}^a$

  $q^w_{conv} \propto u^3_\infty$

- **Radiative Fluxes**

  $T_s = \frac{u^2_\infty}{2C_{p_s}}$;

  $q^w_{rad} = \sigma T^4_s = \frac{u^8_\infty}{(2C_{p_s})^4}$

  $q^w_{rad} \propto u^8_\infty$

  Radiation dominates above 10km/s

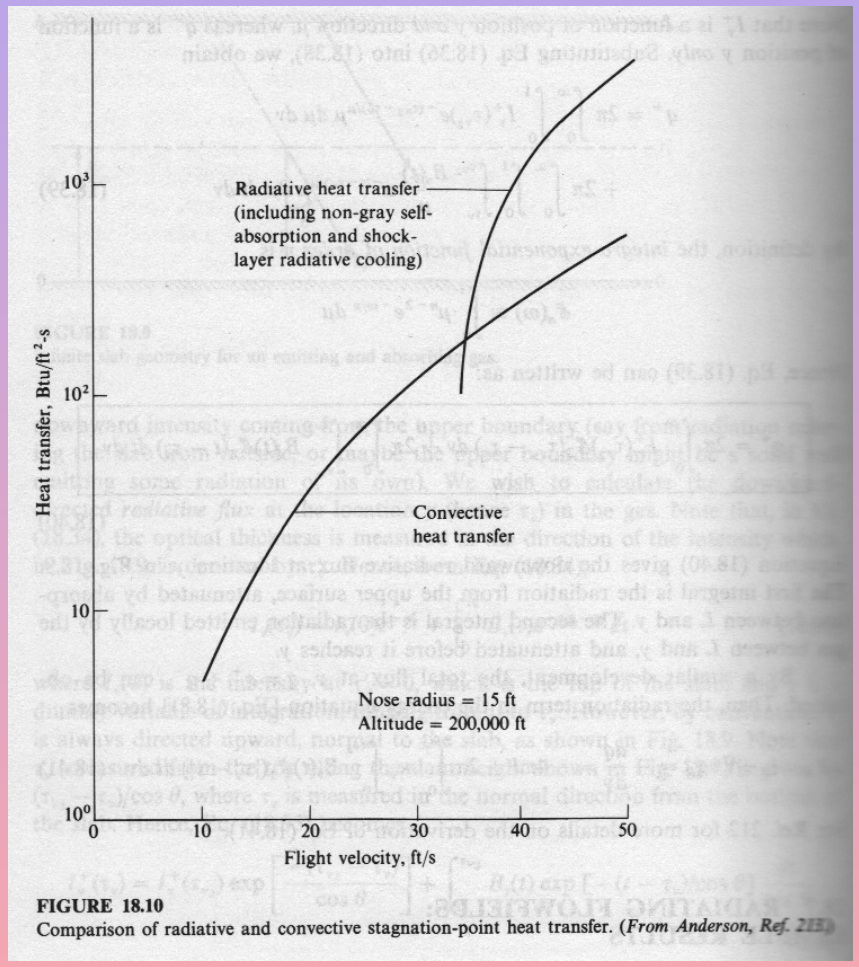


**FIGURE 18.10**
Comparison of radiative and convective stagnation-point heat transfer. (*From Anderson, Ref. 21*)

[a] St: Stanton number

# Boltzmann and Goulard Numbers

Boltzmann number $B_o^{-1}$, Radiation/Convection ratio:

$$B_o^{-1} = \frac{q_{rad}}{q_{conv}} = \frac{\sigma T^4}{\rho u C_p T}$$

Infinite slab approximation[a]. We also have $C_p T \backsimeq u_\infty/2$.

Goulard Number $\Gamma$, Radiative cooling parameter

$$\Gamma = \frac{2q^w_{rad}}{q^w_{conv}} = \frac{2q^w_{rad}}{1/2\rho_\infty u^3_\infty}$$

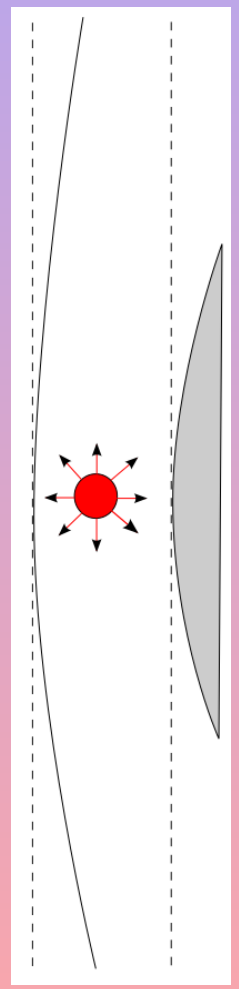

$\sigma$: Stefan-Boltzmann constant

[a] half the radiated power goes upstream, half to the wall

# Optically Thin and Optically Thick Limiting Cases

- **Optically Thin:** $\Gamma_n = \dfrac{4\sigma T_s^4 \alpha \delta}{\rho_\infty u_\infty h_s}$
- **Optically Thick**[a]**:** $\Gamma_k = \dfrac{16\sigma T_s^4 \alpha}{3\rho_\infty u_\infty h_s}$

- $\Gamma < 10^{-3}$: radiation is not important
- $10^{-3} < \Gamma < 10^{-2}$: radiation is important but coupling is not necessary
- $\Gamma > 10^{-2}$: coupling of the radiation to the flowfield is necessary

The absorption coefficient is related to the optical transmissivity such that $T = \exp(-\alpha\delta)$. Transmissivity goes from 100% (optically thin) to 0% (optically thick).

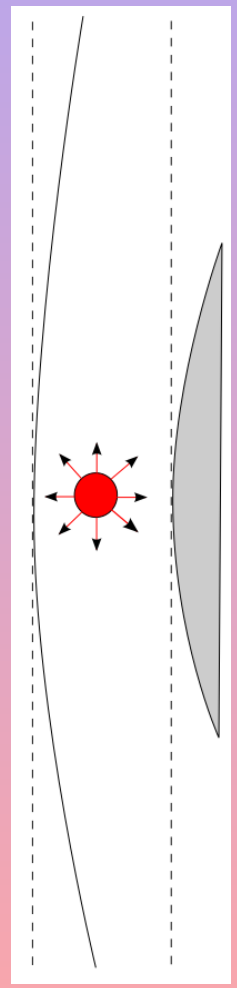

[a] known as the Rosseland limit

# Radiative Transfer Regimes

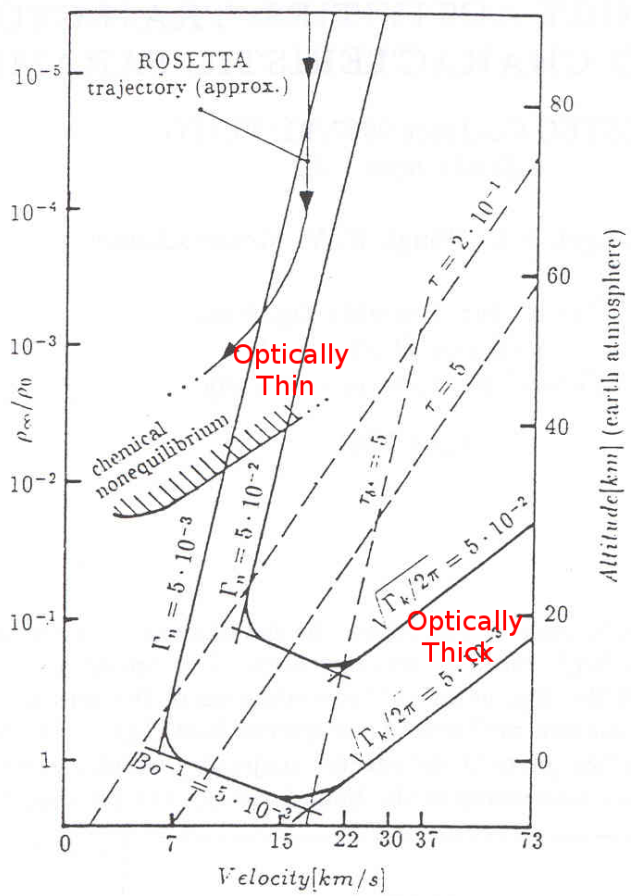


Figure 2: Radiative transfer regimes for a blunt body of 1 ft nose radius, taken from [2]

# Sample Correlated Heat Fluxes for the Huygens Entry

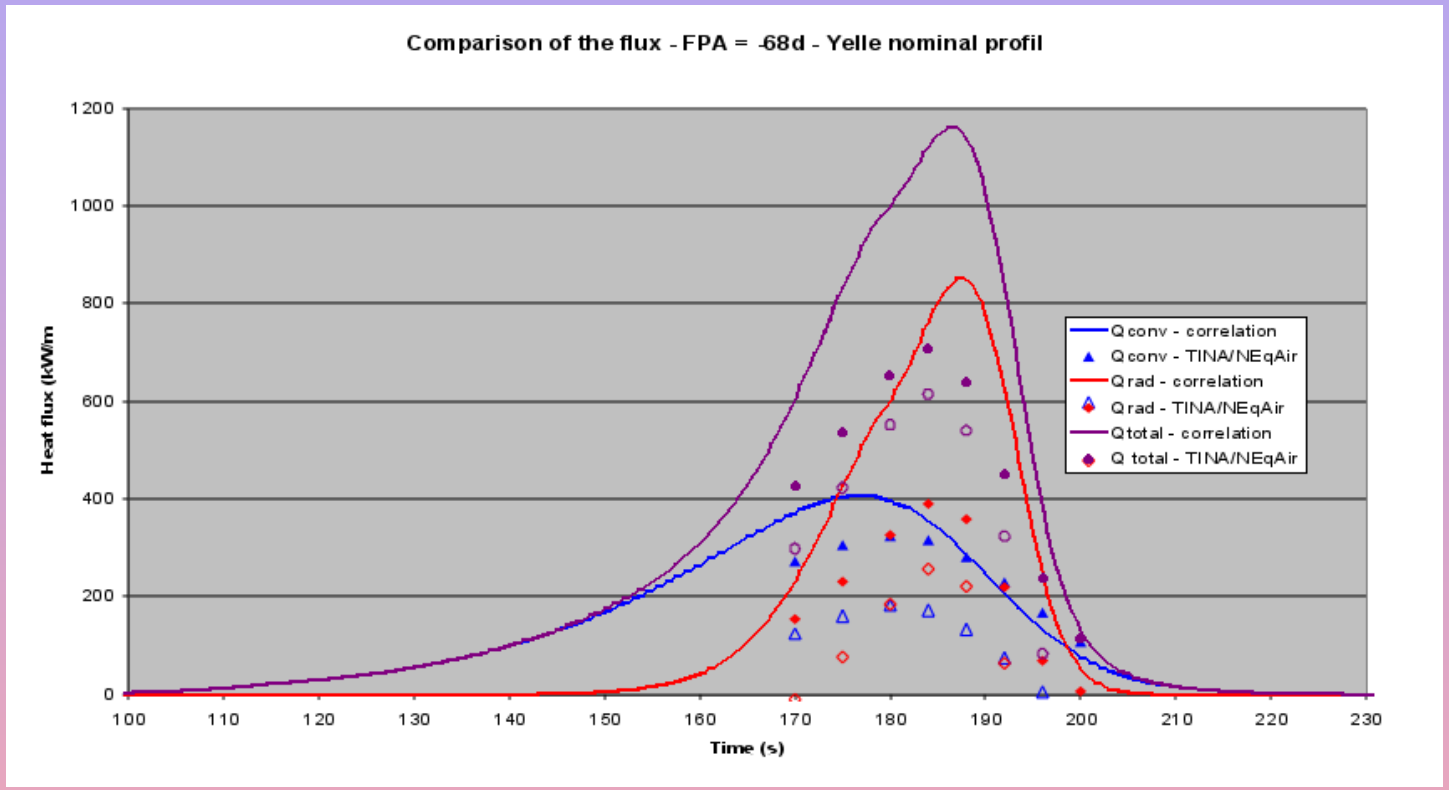


Correlated and simulated convective heat fluxes for the Huygens entry

Engineering correlations allow a first sampling of the spacecraft shape and the selection of an appropriate descent trajectory. Then CFRD simulations can be carried out for specific trajectory points

# Computational Fluid Radiative Dynamics Simulations

- Development of radiative databases providing the spectral-dependent emission $\varepsilon_\nu$ and absorption $\alpha(\nu)$ coefficients for any arbitrary state of the plasma
- Accounting for bound, bound–free (photodissociation, photoionization, photodetachment) and free-free (Bremstrahlung) transitions
- bound-bound transitions include atomic, diatomic and polyatomic transitions
- Radiative transfer equation is then solved over the computational domain

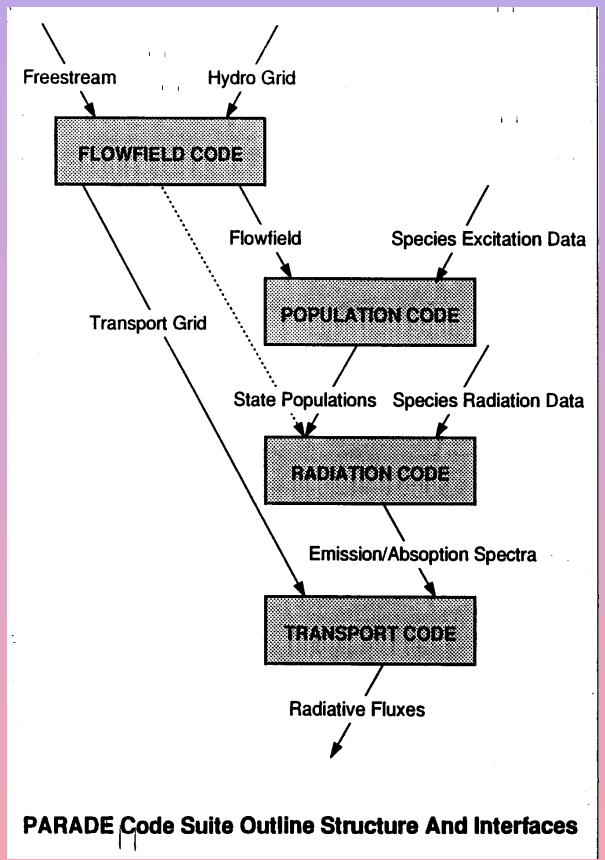

PARADE Code Suite Outline Structure And Interfaces

# Development of Spectral Databases

- atomic and polyatomic transitions typically simulated from external radiative databases (NIST, TopBase, HITRAN)
- diatomic transitions databases are explicitely obtained using appropriate quantum-mechanics models
- continuum radiation calculated from published absorption cross-sections (e.g. TopBase for atomic photoionization), or from semi-empirical to exact cross-sections for molecular continuum cross-sections

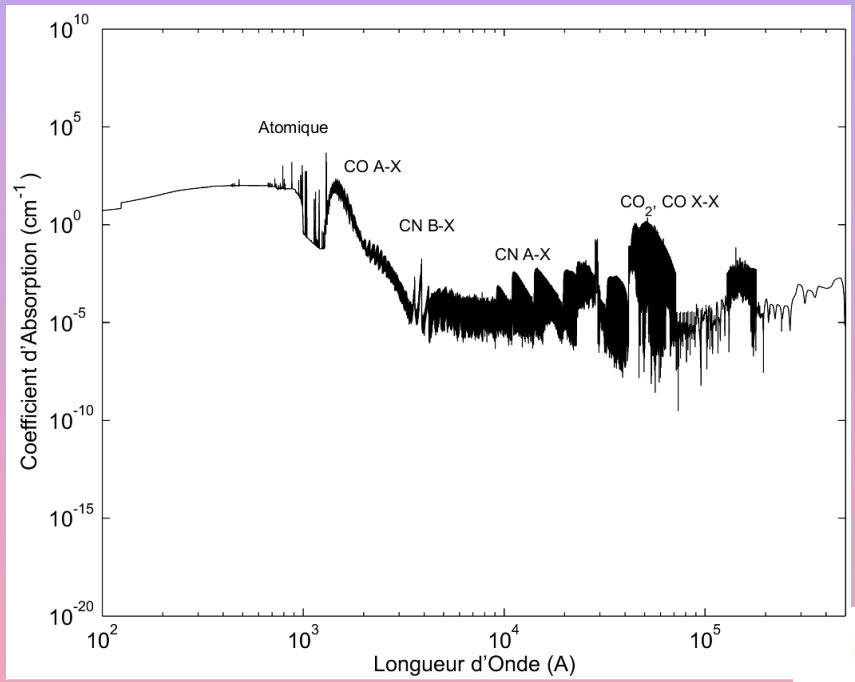


Absorption Coefficient for a 97%$CO_2$–3%$N_2$ Plasma in Thermochemical Equilibrium at 5000K and 1bar

# Line-by-Line Models

- "Collection" of lines which correspond to the overall quantum-allowed radiative transitions between the internal levels of an atom/molecule.
- Selection rules define the quantum-allowed transitions, which must respect angular and spin momentum conservation for atoms and molecules.
- Three key parameters:
  1) Line position considering Planck's Law: $\nu = E_u - E_l/hc$;
  2) Line intensity: $I_\nu = N_u A_{ul} \Delta E_{ul}$;
  3) Line profile: $F(\nu - nu_0)$, Voigt (sum of a Lorentz & Gaussian profile).
- Radiative spectra obtained through the superposition of these overall lines.

# Line-by-Line Models

- "Collection" of lines which correspond to the overall quantum-allowed radiative transitions between the internal levels of an atom/molecule.
- Selection rules define the quantum-allowed transitions, which must respect angular and spin momentum conservation for atoms and molecules.
- Three key parameters:
  1) Line position considering Planck's Law: $\nu = E_u - E_l/hc$;
  2) Line intensity: $I_\nu = N_u A_{ul} \Delta E_{ul}$;
  3) Line profile: $F(\nu - nu_0)$, Voigt (sum of a Lorentz & Gaussian profile).
- Radiative spectra obtained through the superposition of these overall lines.

# Line-by-Line Models

- "Collection" of lines which correspond to the overall quantum-allowed radiative transitions between the internal levels of an atom/molecule.
- Selection rules define the quantum-allowed transitions, which must respect angular and spin momentum conservation for atoms and molecules.
- Three key parameters:
  1) Line position considering Planck's Law: $\nu = E_u - E_l/hc$;
  2) Line intensity: $I_\nu = N_u A_{ul} \Delta E_{ul}$;
  3) Line profile: $F(\nu - nu_0)$, Voigt (sum of a Lorentz & Gaussian profile).
- Radiative spectra obtained through the superposition of these overall lines.

# Line-by-Line Models

- "Collection" of lines which correspond to the overall quantum-allowed radiative transitions between the internal levels of an atom/molecule.
- Selection rules define the quantum-allowed transitions, which must respect angular and spin momentum conservation for atoms and molecules.
- Three key parameters:
  1) Line position considering Planck's Law: $\nu = E_u - E_l/hc$;
  2) Line intensity: $I_\nu = N_u A_{ul} \Delta E_{ul}$;
  3) Line profile: $F(\nu - nu_0)$, Voigt (sum of a Lorentz & Gaussian profile).
- Radiative spectra obtained through the superposition of these overall lines.

# Key Parameters

The fundamental equation for intensity

$$I_\nu = N_u A_{ul} \Delta E_{ul} F(\nu - \nu_0)$$

can be decoupled in the following variables :

- $N_u$ : Level populations :
  Either a Boltzmann equilibrium distribution, either through Collisional-Radiative nonequilibrium models
- $A_{ul}$ : Transition probabilities (Einstein Coefficients):
  From "ab-initio" or measured transition moments
- $\Delta E_{ul}$ : Level energies:
  Fitting and extrapolation of experimentally determined data
- $F(\nu - \nu_0)$ : Line profile:
  Voigt profiles accounting for Doppler and Collisional broadening (depends on the local conditions of the plasma)

# Key Parameters

The fundamental equation for intensity

$$I_\nu = N_u A_{ul} \Delta E_{ul} F(\nu - \nu_0)$$

can be decoupled in the following variables :

- $N_u$ : Level populations :

  Either a Boltzmann equilibrium distribution, either through Collisional-Radiative nonequilibrium models

- $A_{ul}$ : Transition probabilities (Einstein Coefficients):

  From "ab-initio" or measured transition moments

- $\Delta E_{ul}$ : Level energies:

  Fitting and extrapolation of experimentally determined data

- $F(\nu - \nu_0)$ : Line profile:

  Voigt profiles accounting for Doppler and Collisional broadening (depends on the local conditions of the plasma)

# Rotational-Vibrational Level Energies of Diatomic Molecules

$$
\begin{aligned}
E_{e,v,J} &= T_e + G(v) + B_v(J) \\
&= T_e + \omega_e (v+1/2) - \omega_e x_e (v+1/2)^2 + \omega_e y_e (v+1/2)^3 + \ldots \\
&+ \left[ B_e - \alpha_e (v+1/2) + \gamma_e (v+1/2)^2 + \ldots \right] [J(J+1)] \\
&- [D_e + \beta_e (v+1/2) + \ldots] [J(J+1)]^2 + \ldots
\end{aligned}
$$

In the compact Dunham matrix form (strictly valid only for $^1\Sigma$ states):

$$E_{e,v,J} = \sum_{i,j} Y_{ij} (v+1/2)^i [F(J)]^j,$$

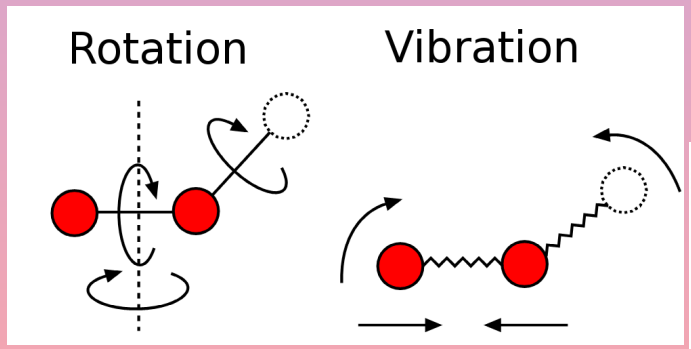


Molecular vibrational and rotational levels

# Potential Reconstruction Methods

- Potential reconstruction methods allow determining the radial wavefunction for the molecular vibrational levels.
- They also incidentally allow more accurate representations of near-dissociative levels, where polynomial expansions are no longer valid.

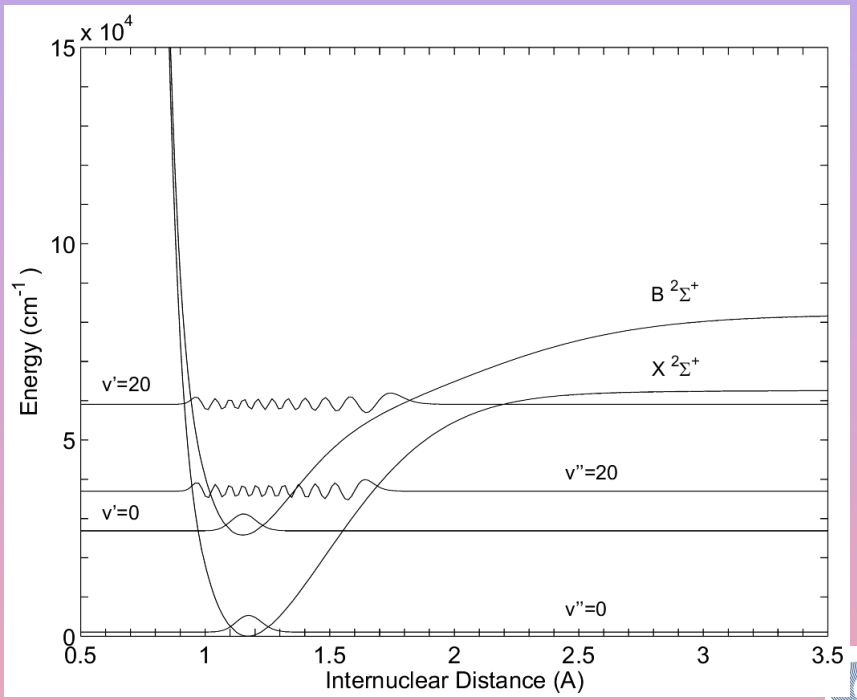


Sample RKR calculation for the CN Violet system

# One Sample Application

- Calculation of the vibrational levels for the $N_2(X^1\Sigma)$ ground state.
- Traditional polynomial expansions predict $v_{max}$=46.
- A more rigorous RKR potential reconstruction method yields $v_{max}$=61.

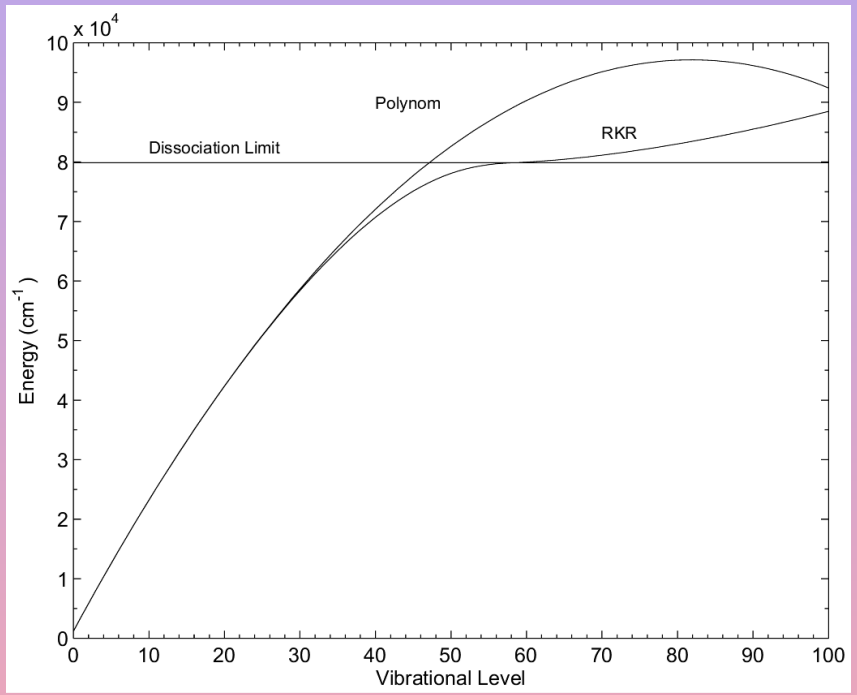


$N_2(X^1\Sigma)$ Level energies calculated using a second order polynomial expansion, and the RKR method

# Fine-structure Effects (1/4)

- Fine-strucure effects like spin splitting and $\Lambda$–Doubling for homonuclear molecules, split one single line into multiplet lines with energies very close one to another.
- Nuclear momentum is named as $\Sigma$, $\Pi$, $\Delta$, etc..,. for $\Lambda = 0, 1, 2$
- The level energies expressions for spin splitted lines are summarized next

# Fine-structure Effects (2/4)

- Singlet States with $\Lambda \neq 0$

$$F_v(J) = B_v(J(J+1)) + (A_v - B_v)\Lambda^2$$

- Doublet States

$$F_{3/2}(J \geq 1) = B_v \left[ \begin{array}{l} \left(J+\frac{1}{2}\right)^2 - \Lambda^2 \\ -\frac{1}{2}\left(4\left(J+\frac{1}{2}\right)^2 + Y_v(Y_v-4)\Lambda^2\right)^{\frac{1}{2}} \end{array} \right] - D_v J^4$$

$$F_{1/2}(J \geq 0) = B_v \left[ \begin{array}{l} \left(J+\frac{1}{2}\right)^2 - \Lambda^2 \\ +\frac{1}{2}\left(4\left(J+\frac{1}{2}\right)^2 + Y_v(Y_v-4)\Lambda^2\right)^{\frac{1}{2}} \end{array} \right] - D_v (J+1)^4$$

# Fine-structure Effects (3/4)

- $^3\Sigma$ Triplet States

$$
\begin{aligned}
{}^3\Sigma_2(J \geq 2) &= B_v(J(J+1)) - D_v(J(J+1))^2 - \left( \lambda_v - B_v + \tfrac{1}{2}\gamma_v \right) \\
&\quad - \left[ \left(\lambda_v - B_v + \tfrac{1}{2}\gamma_v\right)^2 + 4J(J+1)\left(B_v - \tfrac{1}{2}\gamma_v\right)^2 \right]^{\frac{1}{2}} \\
{}^3\Sigma_1(J \geq 1) &= B_v(J(J+1)) - D_v(J(J+1))^2 \\
{}^3\Sigma_0(J \geq 0) &= B_v(J(J+1)) - D_v(J(J+1))^2 - \left( \lambda_v - B_v + \tfrac{1}{2}\gamma_v \right) \\
&\quad + \left[ \left(\lambda_v - B_v + \tfrac{1}{2}\gamma_v\right)^2 + 4J(J+1)\left(B_v - \tfrac{1}{2}\gamma_v\right)^2 \right]^{\frac{1}{2}}
\end{aligned}
$$

# Fine-structure Effects (4/4)

- $^3\Pi$ Triplet States

$$
{}^3\Pi_2(J \geq 2) = B_v \left[ \begin{array}{c} J(J+1) - \sqrt{y_1 + 4J(J+1)} \\ -\frac{2}{3}\frac{y_2 - 2J(J+1)}{y_1 + 4J(J+1)} \end{array} \right] - D_v \left( J - \frac{1}{2} \right)^4
$$

$$
{}^3\Pi_1(J \geq 1) = B_v \left[ J(J+1) + \frac{4}{3}\frac{y_2 - 2J(J+1)}{y_1 + 4J(J+1)} \right] - D_v \left( J + \frac{1}{2} \right)^4
$$

$$
{}^3\Pi_0(J \geq 0) = B_v \left[ \begin{array}{c} J(J+1) + \sqrt{y_1 + 4J(J+1)} \\ -\frac{2}{3}\frac{y_2 - 2J(J+1)}{y_1 + 4J(J+1)} \end{array} \right] - D_v \left( J + \frac{3}{2} \right)^4
$$

with

$$
y_1 = Y_v(Y_v - 4) + \frac{4}{3} \qquad y_2 = Y_v(Y_v - 1) - \frac{4}{9} \qquad Y_v = \frac{A_v}{B_v}
$$

# Selection Rules for Atoms

| | Transitions E1 | Transitions M1 | Transitions E2 |
|---|---|---|---|
| | **Tous types de couplages** | | |
| 1 | $\Delta J = 0, \pm 1$ (sauf $0 \nleftrightarrow 0$) | $\Delta J = 0, \pm 1$ (sauf $0 \nleftrightarrow 0$) | $\Delta J = 0, \pm 1, \pm 2$ (sauf $0 \nleftrightarrow 0$, $\frac{1}{2} \nleftrightarrow \frac{1}{2}$, $1 \nleftrightarrow 1$) |
| 2 | $\Delta M = 0, \pm 1$ (sauf $0 \nleftrightarrow 0$ lorsque $J = 0$) | $\Delta M = 0, \pm 1$ (sauf $0 \nleftrightarrow 0$) lorsque $J = 0$) | $\Delta M = 0, \pm 1, \pm 2$ |
| 3 | changement de parité | parité identique | parité identique |
| 4[1] | transition d'un électron avec $\Delta l = \pm 1$, $\Delta n$ arbitraire | pas de changement dans la configuration électronique, soit pour tous les électrons: $\Delta l = 0$, $\Delta n = 0$ | pas de changement dans la configuration électronique, ou bien pour un électron: $\Delta l = 0, \pm 2$, $\Delta n$ arbitraire |
| | **Couplage L–S** | | |
| 5 | $\Delta S = 0$ | $\Delta S = 0$ | $\Delta S = 0$ |
| 6 | $\Delta L = 0, \pm 1$ (sauf $0 \nleftrightarrow 0$) | $\Delta L = 0$, $\Delta J = \pm 1$ | $\Delta L = 0, \pm 1, \pm 2$ (sauf $0 \nleftrightarrow 0$, $0 \nleftrightarrow 1$) |

[1] Lorsque l'interaction de configuration est négligeable.

# Selection Rules for Molecules

| | |
|---|---|
| transition entre niveaux de rotation | $\Delta J = 0, \pm 1$ (sauf $0 \nleftrightarrow 0$) |
| parité des niveaux de rotation | $+ \leftrightarrow -$ permis<br>$+ \nleftrightarrow +, - \nleftrightarrow -$ interdits |
| branches de rotation $Q(\Delta J = 0)$ | $e \leftrightarrow f$ permis<br>$e \leftrightarrow e, f \leftrightarrow f$ interdits |
| branches de rotation $P, R(\Delta J = \pm 1)$ | $e \leftrightarrow e, f \leftrightarrow f$ permis<br>$e \nleftrightarrow f$ interdits |
| molecules homonucleaires | $s \leftrightarrow s, a \leftrightarrow a$ permis<br>$s \nleftrightarrow a$ interdits |
| noyaux de même charge | $g \leftrightarrow u$ permis<br>$g \leftrightarrow g, u \leftrightarrow u$ interdits |

# Transition Probabilities (1/2)

Transition probability $A_{ul}$ decomposed into vibronic and rotational product

$$A_{ul} = A^{e'v'}_{e''v''} \cdot A^{\Lambda' J'}_{\Lambda'' J''}$$

with

$$A^{e'v'}_{e''v''} = \frac{64\pi^4 \overline{\nu}^3}{3hc^3} \frac{(2 - \delta_{0,\Lambda'+\Lambda''})}{(2 - \delta_{0,\Lambda'})} \left(R_e^{v'v''}\right)^2$$

and

$$\left(R_e^{v'v''}\right)^2 \cong \frac{\sum \left(R_e^{v'v''}\right)^2}{(2 - \delta_{0,\Lambda'+\Lambda''})(2S+1)}$$

The vibronic transition moment being obtained from the integration of the electronic transition moment $R_e(r)$ and the upper and lower states wavefunctions

$$\left(R_e^{v'v''}\right)^2 = \left(\int \psi_{v'}(r) R_e(r) \psi_{v''}(r) dr\right)^2$$

# Transition Probabilities (2/2)

The rotational transiton probability is given by the Hönl-London factors

$$A^{\Lambda' J'}_{\Lambda'' J''} = \frac{S^{\Lambda' J'}_{\Lambda'' J''}}{2J' + 1}$$

which depend on the type of rotation-electronic motion coupling (Hund Case), and the type of electronic transition (${}^n\Lambda \leftrightarrow {}^n\Lambda$).
We use the normalization rule

$$\sum_{J''} S^{\Lambda' J'}_{\Lambda'' J''}(J') = (2J' + 1)$$

and we may then write

$$A_{ul} = \frac{64\pi^4 \overline{\nu}^3}{3hc^3} \frac{\sum \left( R_e^{v' v''} \right)^2}{(2 - \delta_{0,\Lambda'})(2S + 1)} \frac{S^{\Lambda' J'}_{\Lambda'' J''}}{2J' + 1}$$

# Voigt Lineshape Calculation Method

- Line broadening mechanisms from Doppler or collision effects (Lorentz lineshape).
- Objective: To calculate the most accurate Voigt lineshape (convolution of Doppler and Lorentz lineshapes) utilizing a minimum number of points.
- Input parameters: line position, emission/absorption coefficient, Doppler/Lorentz FWHM.
- Starting point: Analytical expression of Whiting, updated by Olivero (JQSRT, Vol. 17, 1977, pp. 233).
- Definition of low-resolution lines (5 to 11 grid points) and high-resolution lines (typically more than 20 points).

# Definition of Strong and Weak Lines

- Definition of strong, weak, and very weak lines.
- In the "pseudo-continuum" approach, only strong lines and uncovered weak lines are calculated explicitly. Other lines are added as a continuum.

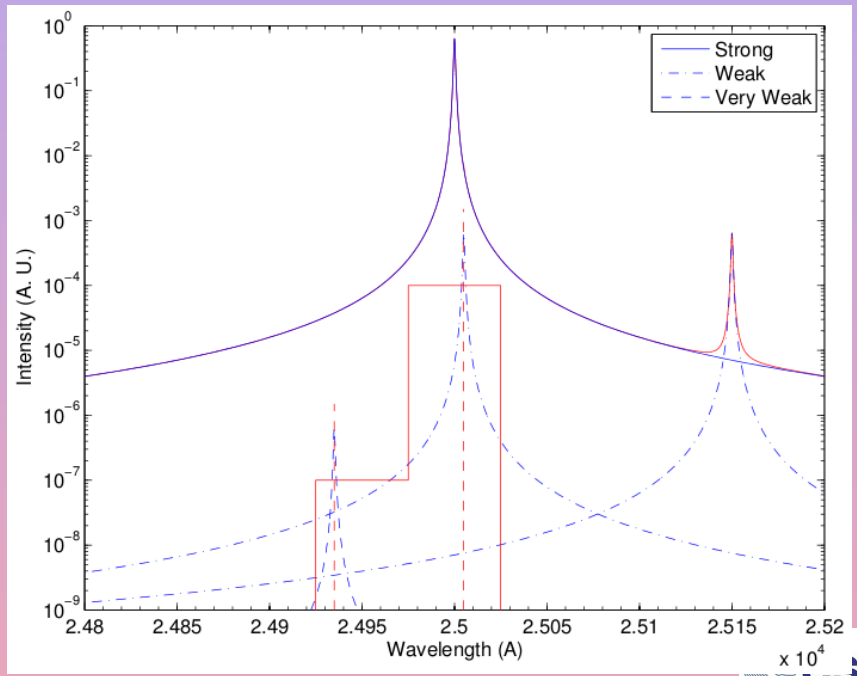


Sample strong, weak, and very weak lines (with thresholds $10^3$ and $10^6$)

# Sample Calculation for the CN Violet System

- Here, only the strong lines for diagonal transitions are explicitly calculated.
- The "pseudo-continuum" extends below.
- Significant savings in calculation times and spectral grid sizes can be achieved (Lino da Silva, JQSRT 2007)

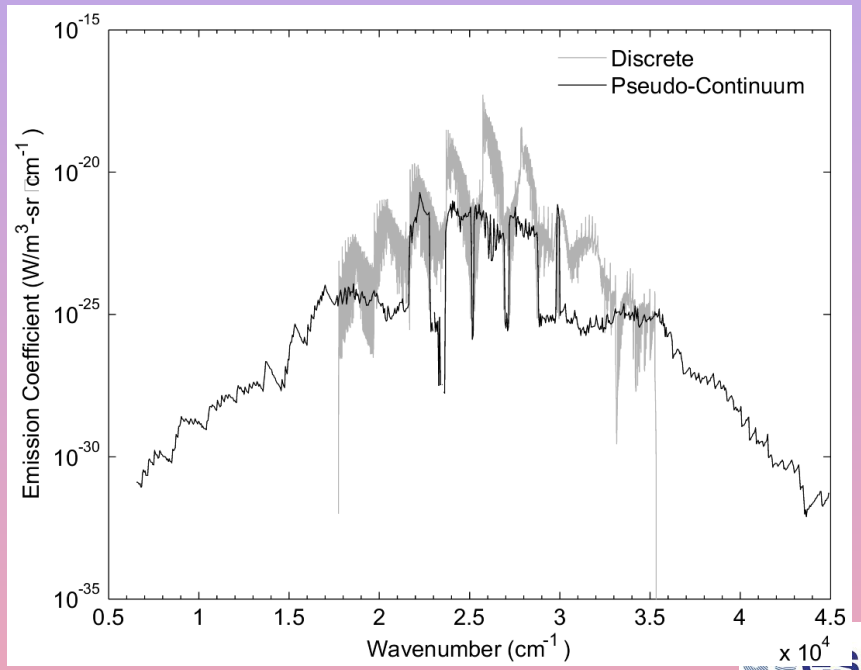


Calculation of the molecular CN Violet System using the hybrid line-by-line/pseudo-continuum approach.

# Elementary Radiative Processes

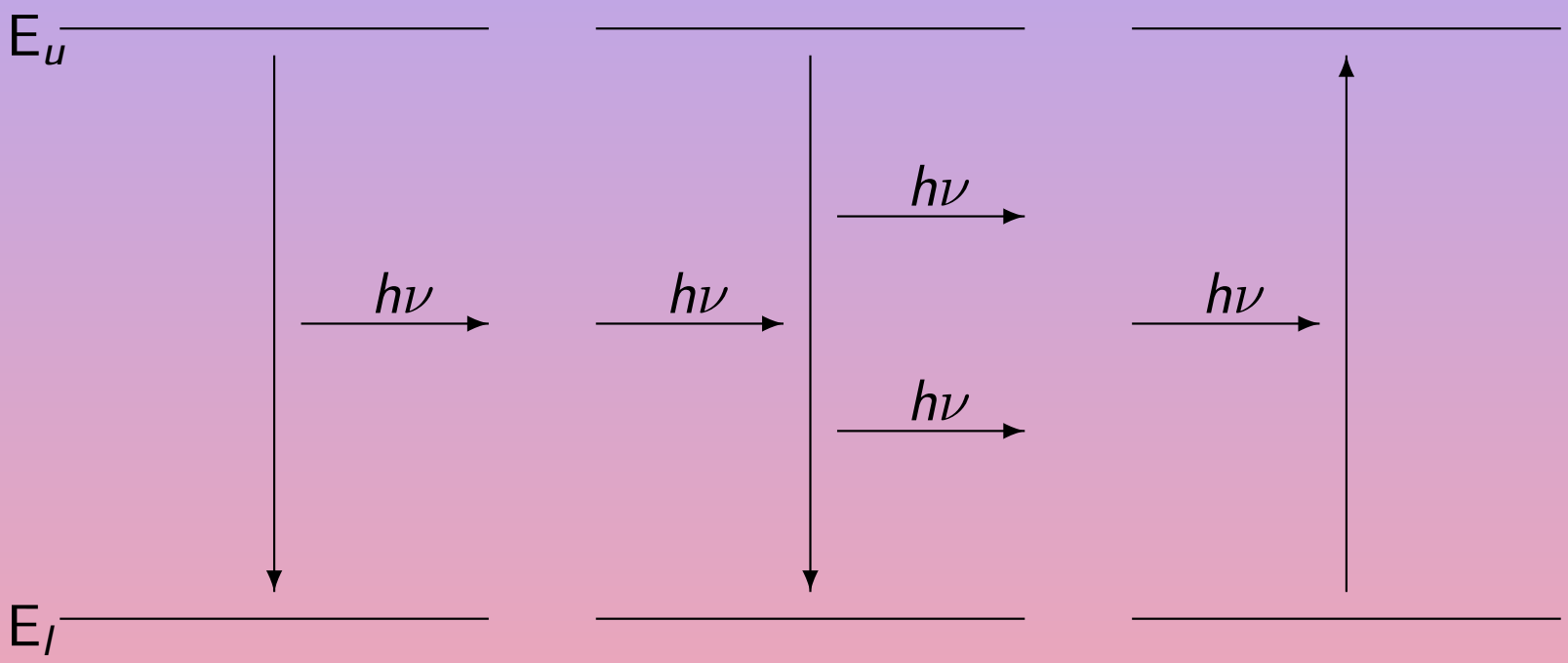


spontaneous emission induced emission absorption

$$\frac{\partial N_u}{\partial t} = -N_u A_{ul} \qquad \frac{\partial N_u}{\partial t} = -N_u B_{ul} u_\nu \qquad \frac{\partial N_l}{\partial t} = -N_u B_{ul} u_\nu$$

# Derivation of the Radiative Transfer Equation (RTE) (1/2)

Summing the three processes we have

$$\frac{\partial N_u}{\partial t} = -N_u A_{ul} + [N_u B_{ul} - N_u B_{ul}] u_\nu$$

In Radiative equilibrium the net variation is 0, and radiation is given by the Planck Blackbody Law

$$u_\nu^o(T) = \frac{8\pi h\nu^3}{c^3} \left[ \exp\left( -\frac{h\nu}{k_B T} \right) - 1 \right]^{-1}$$

we have

$$g_l B_{lu} = g_u B_{ul}$$
$$\frac{A_{ul}}{B_{ul}} = \frac{8\pi h\nu^3}{c^3}$$

# Derivation of the Radiative Transfer Equation (RTE) (2/2)

Integrating the expressions of the previous slide in volume from we obtain the classical RTE equation:

$$\cos\theta \frac{dL_\nu}{dz} = \varepsilon_\nu - \alpha_\nu L_\nu$$

with

$$\varepsilon_\nu = \frac{n_u A_{ul} h\nu}{4\pi}$$

$$\alpha(\nu) = \left( n_u - \frac{g_u}{g_l} n_l \right) B_{ul} \frac{h\nu}{c}$$

which becomes the Beer-Lambert Law in 1D coordinates:

$$\frac{dI_\nu}{dl} = \varepsilon - \alpha(\nu) I_\nu$$

and after integration:

$$I_\nu = \frac{\varepsilon}{\alpha(\nu)} [1 - \exp(-\alpha(\nu) l)]$$

# Detailed Balancing Principle for Radiation

- Bound-Bound Transitions

$$\frac{\varepsilon_\nu}{\alpha_\nu} = \frac{2h\nu^3}{c^2}\left(\frac{g_u n_l}{g_l n_e} - 1\right)^{-1}$$

- Bound-Free Transitions

$$\frac{\sigma_{bf}(\nu)}{\sigma_{fb}(\nu)} = \frac{1}{2}\left(\frac{m_e v_e c}{h\nu}\right)^2 \frac{g_+ g_e}{g_n}$$

- Free-Free Transitions

$$\frac{\varepsilon_\nu}{\alpha_\nu} = \frac{2h\nu^3}{c^2}\left[\exp\left(\frac{h\nu}{k_B T_e}\right) - 1\right]^{-1}$$

# Detailed Balancing Principle for Radiation

- Bound-Bound Transitions

$$\frac{\varepsilon_\nu}{\alpha_\nu} = \frac{2h\nu^3}{c^2}\left(\frac{g_u n_l}{g_l n_e} - 1\right)^{-1}$$

- Bound-Free Transitions

$$\frac{\sigma_{bf}(\nu)}{\sigma_{fb}(\nu)} = \frac{1}{2}\left(\frac{m_e v_e c}{h\nu}\right)^2 \frac{g_+ g_e}{g_n}$$

- Free-Free Transitions

$$\frac{\varepsilon_\nu}{\alpha_\nu} = \frac{2h\nu^3}{c^2}\left[\exp\left(\frac{h\nu}{k_B T_e}\right) - 1\right]^{-1}$$

# Detailed Balancing Principle for Radiation

- Bound-Bound Transitions

$$\frac{\varepsilon_\nu}{\alpha_\nu} = \frac{2h\nu^3}{c^2}\left(\frac{g_u n_l}{g_l n_e} - 1\right)^{-1}$$

- Bound-Free Transitions

$$\frac{\sigma_{bf}(\nu)}{\sigma_{fb}(\nu)} = \frac{1}{2}\left(\frac{m_e v_e c}{h\nu}\right)^2 \frac{g_+ g_e}{g_n}$$

- Free-Free Transitions

$$\frac{\varepsilon_\nu}{\alpha_\nu} = \frac{2h\nu^3}{c^2}\left[\exp\left(\frac{h\nu}{k_B T_e}\right) - 1\right]^{-1}$$

# Ray-Tracing Methods for Space-Related Heat Transfer Analysis

- Ray-Tracing: An exact method for determining the quantities of photons which irradiate a surface.
-

$$q_\nu = \int_{-\pi/2}^{\pi/2} \int_0^{\pi} I_\nu(\theta,\phi) cos\theta \sin\theta d\theta d\phi$$

$$I_\nu = \frac{\varepsilon}{\alpha'} [1 - \exp(-\alpha I(\theta))]$$

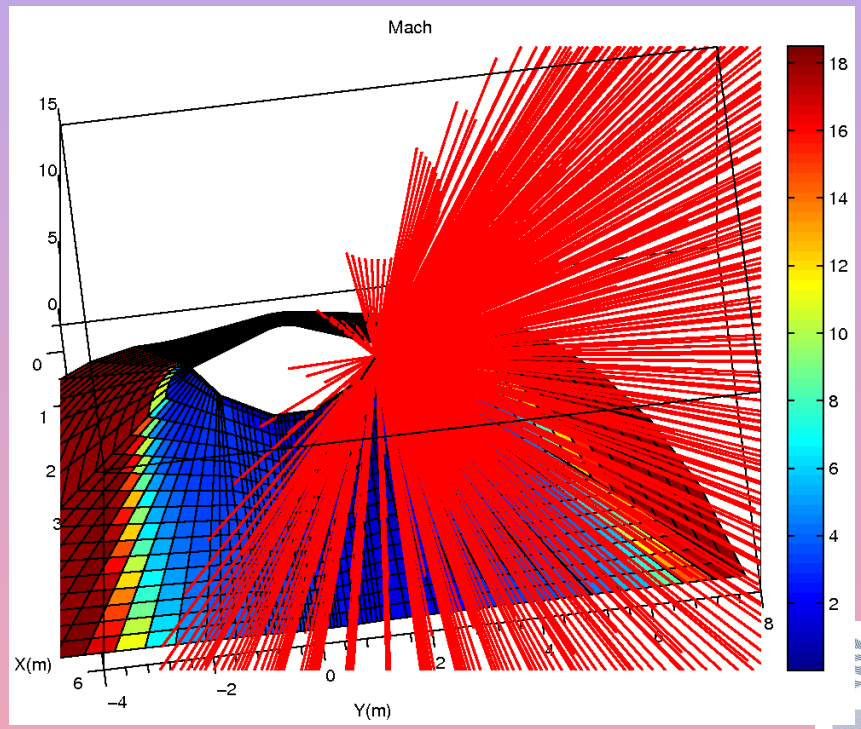


- Ray-tracing considers full 3D geometries, with the possibility of simpler 2D/1D slab geometries.

# Ray-Tracing Methods for Space-Related Heat Transfer Analysis

- Ray-Tracing: An exact method for determining the quantities of photons which irradiate a surface.
-

$$q_\nu = \int_{-\pi/2}^{\pi/2} \int_0^{\pi} I_\nu(\theta, \phi) cos\theta \sin\theta d\theta d\phi$$

$$I_\nu = \frac{\varepsilon}{\alpha'} [1 - \exp(-\alpha I(\theta))]$$

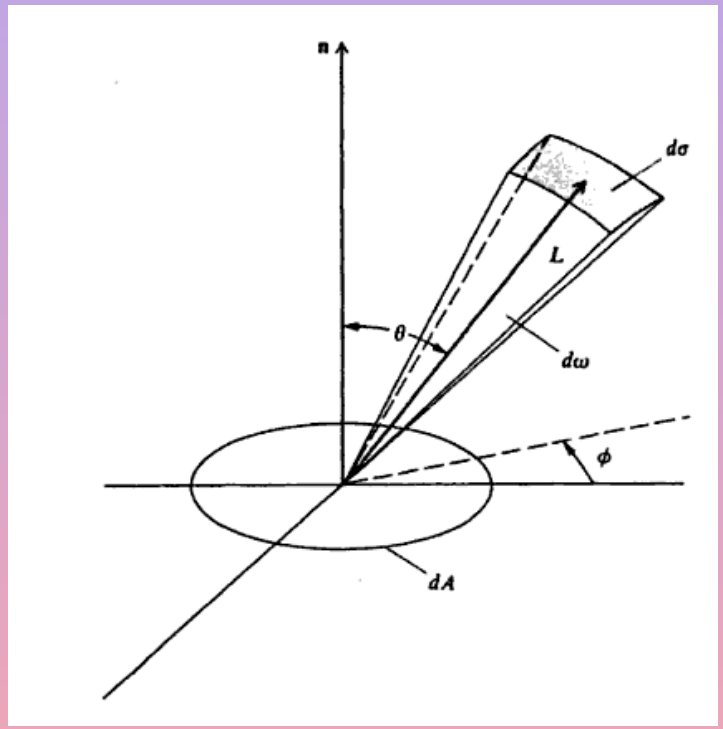


- Ray-tracing considers full 3D geometries, with the possibility of simpler 2D/1D slab geometries.

# Ray-Tracing Methods for Space-Related Heat Transfer Analysis

- Ray-Tracing: An exact method for determining the quantities of photons which irradiate a surface.
-

$$q_\nu = \int_{-\pi/2}^{\pi/2} \int_0^{\pi} I_\nu(\theta, \phi) cos\theta \sin\theta d\theta d\phi$$

$$I_\nu = \frac{\varepsilon}{\alpha'} [1 - \exp(-\alpha I(\theta))]$$

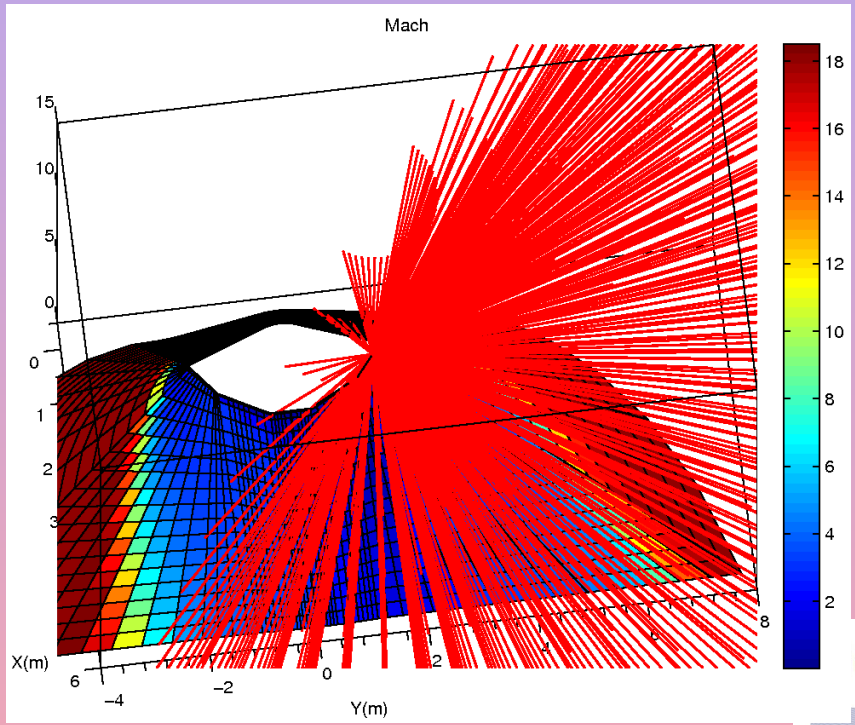


- Ray-tracing considers full 3D geometries, with the possibility of simpler 2D/1D slab geometries.

# Ray-Tracing Methods for Space-Related Heat Transfer Analysis

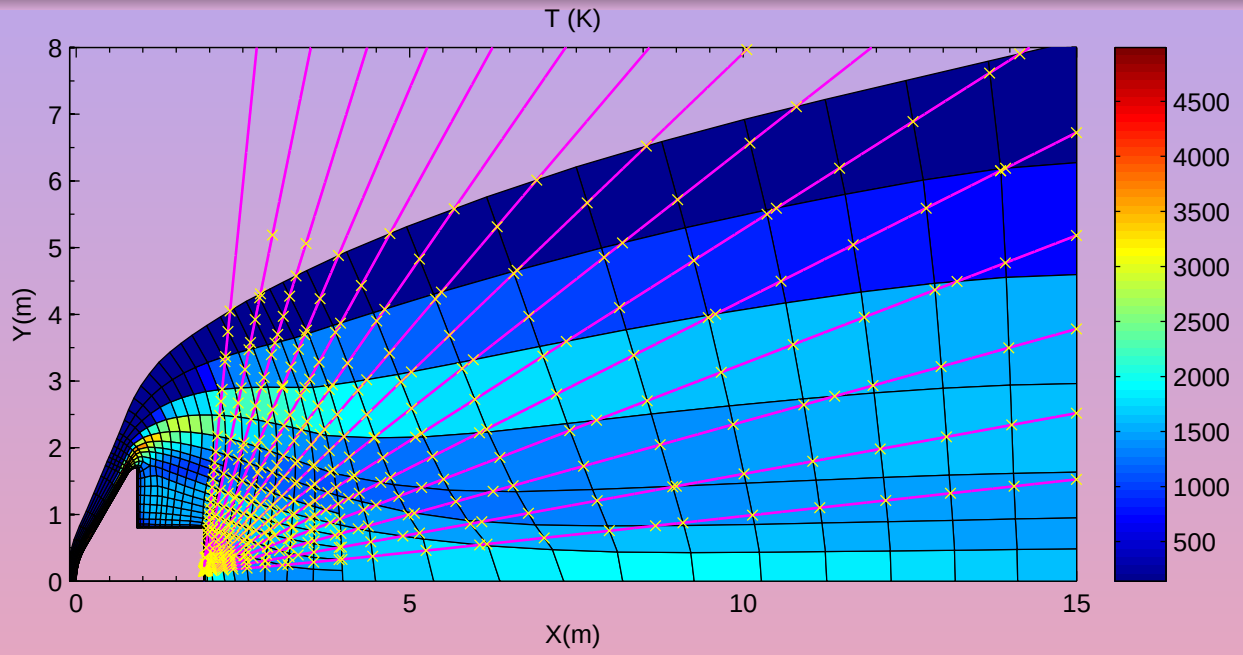


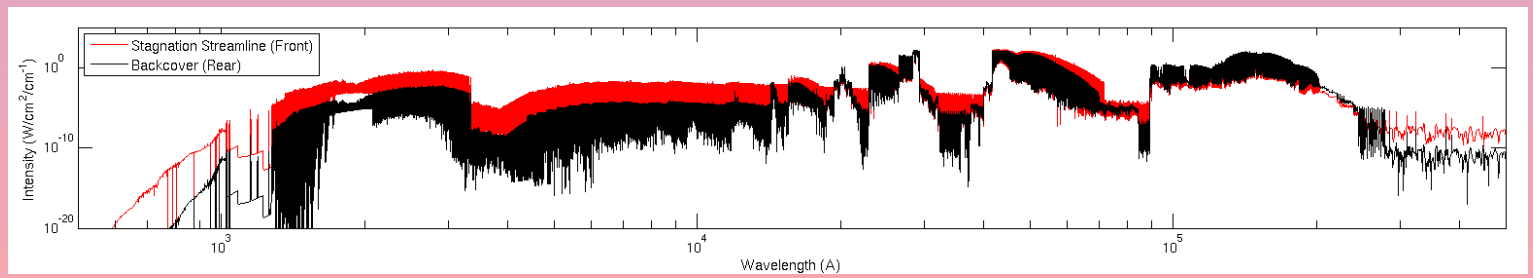


Complex flow geometries with millions of molecular spectral lines

# Case Studies

# Huygens Titan Entry (2005)

- 60 half angle blunted cone
- Base diameter: 2.7 m
- Nose radius: 1.25 m
- Entry module mass: 318.62 kg
- Aerodynamic databases developed by EADS between 1991 and 1995.

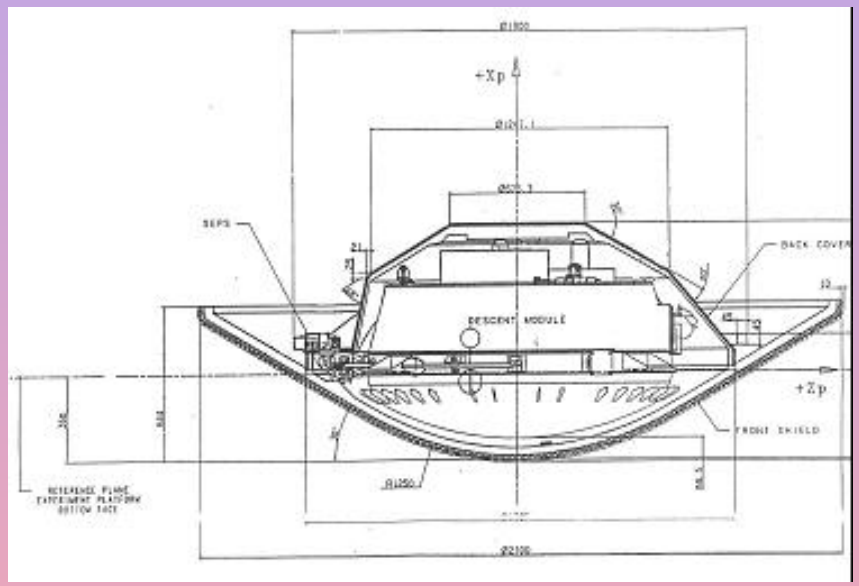

# Huygens Heat Fluxes: Dispersions associated to Cd uncertainties

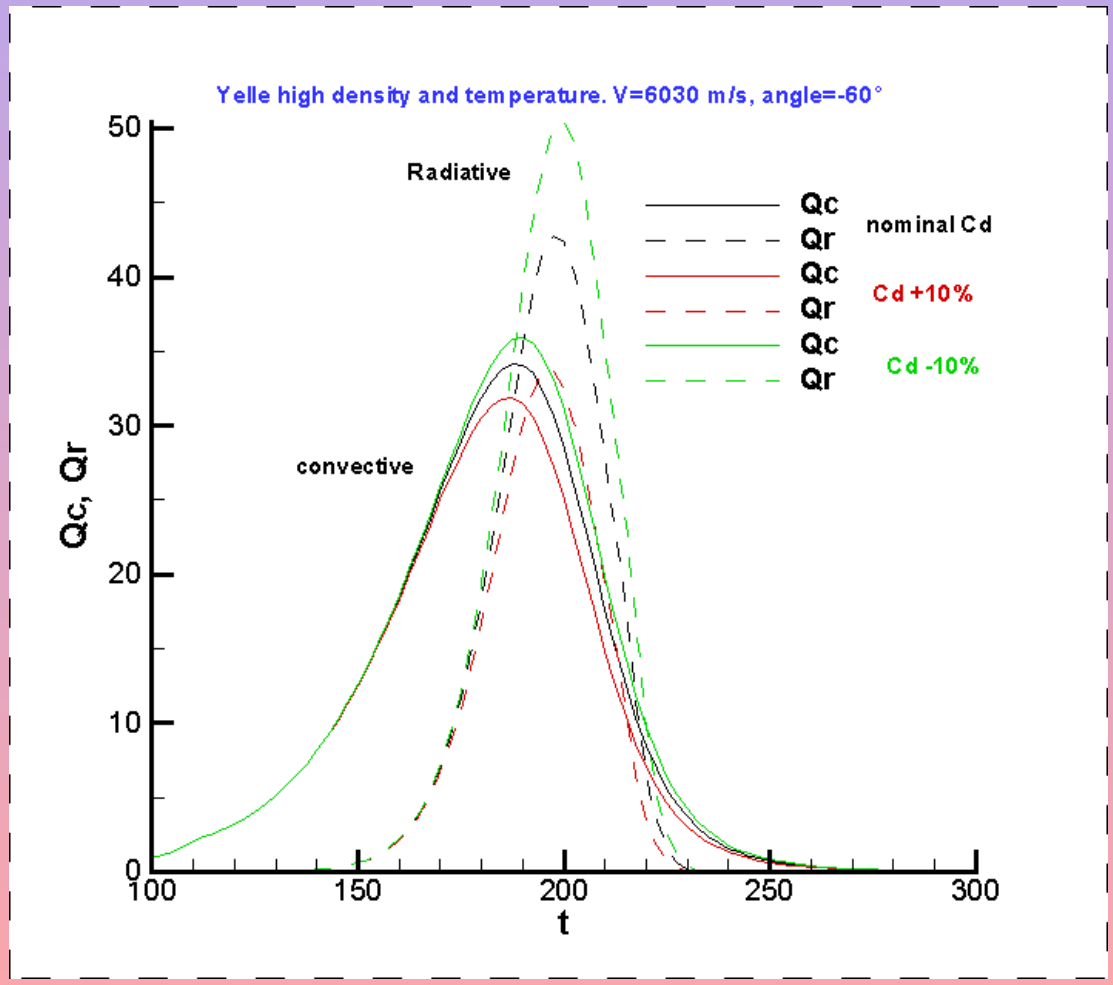

# Huygens Heat Fluxes: Nominal Yelle Atmospheric Profile

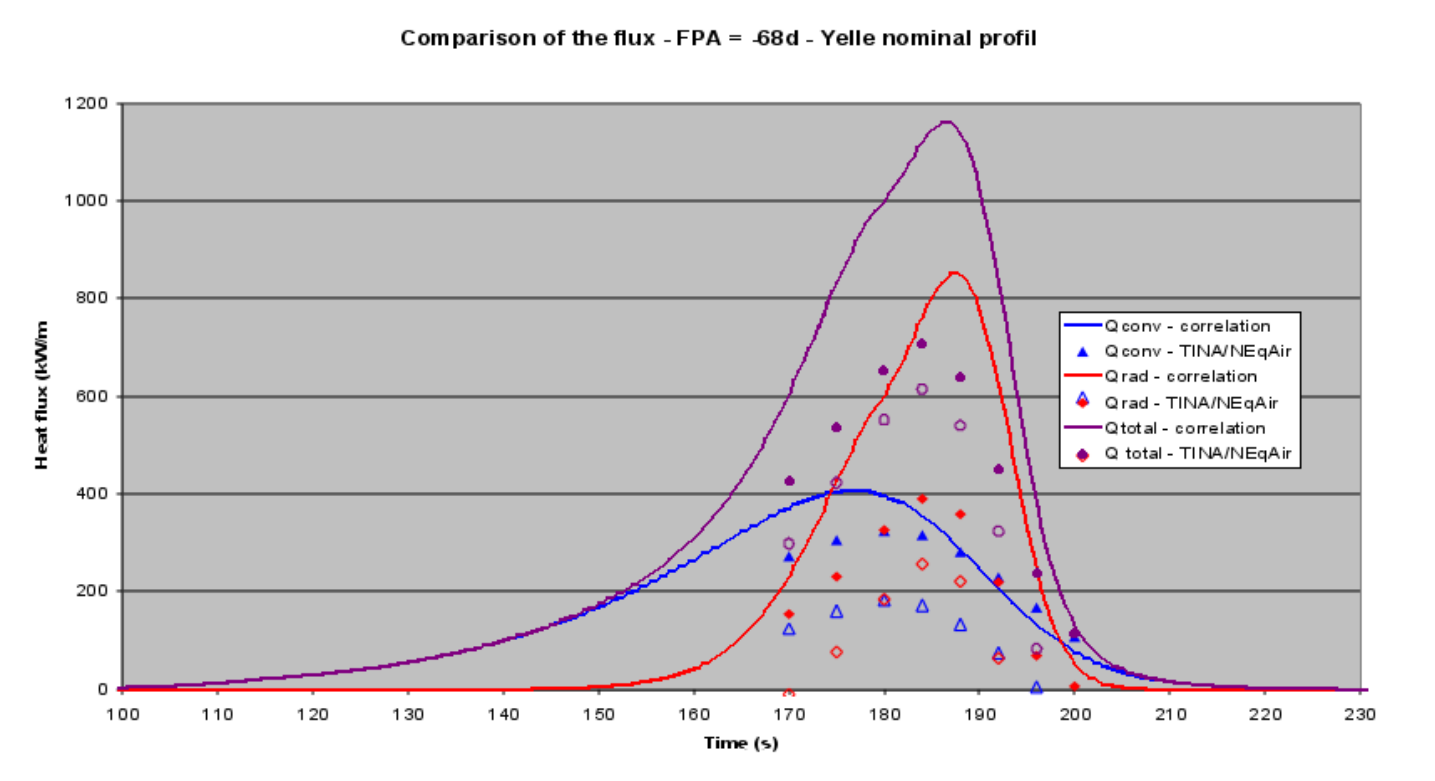


- Titan Composition: 95% $N_2$–5% $CH_4$
- Important Radiator species CN produced in the shock layer. correlations do not work anymore.

# Huygens Heat Fluxes: Nominal Yelle Atmospheric Profile

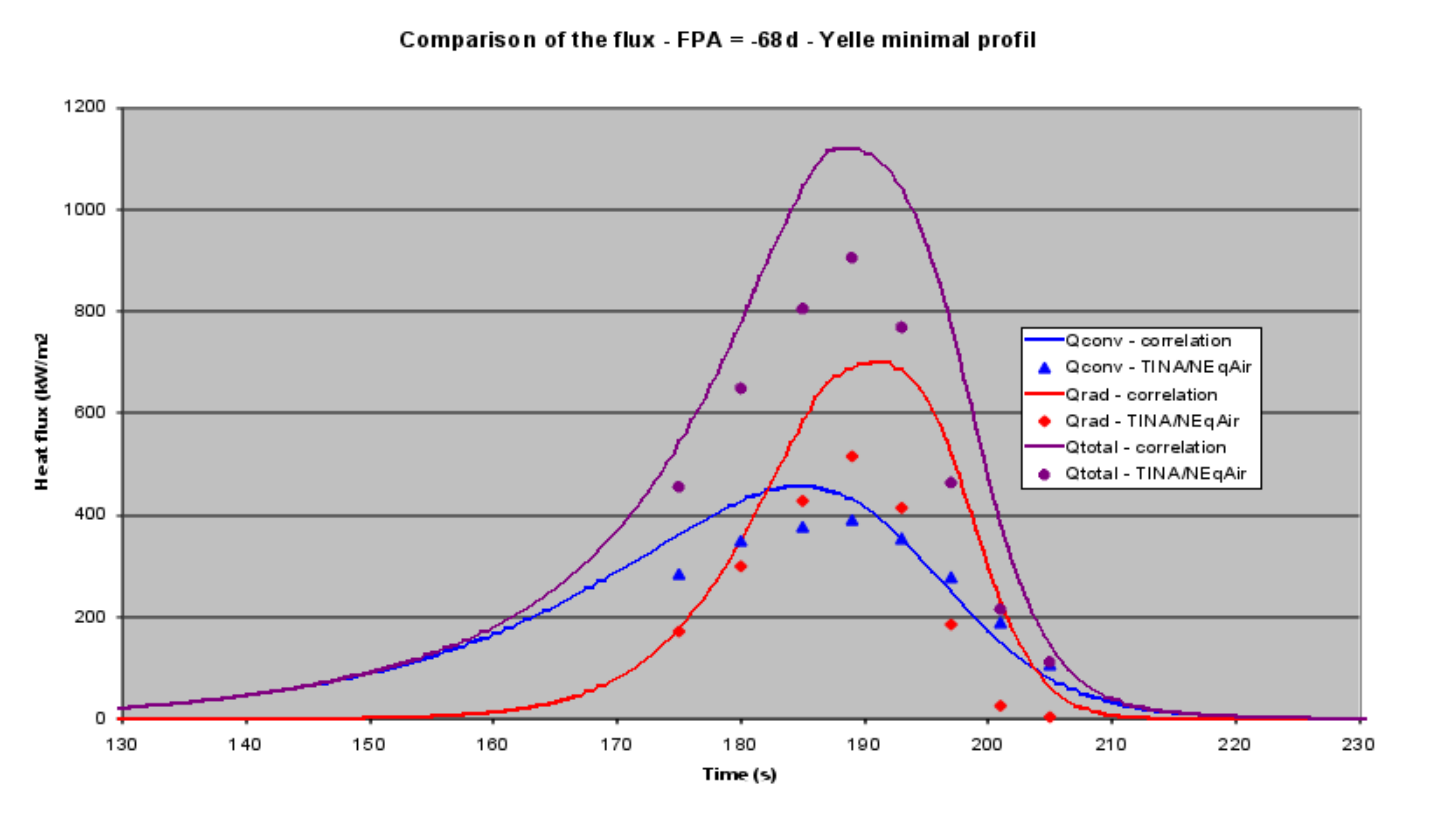


- Titan Composition: 95% $N_2$–5% $CH_4$
- Important Radiator species CN produced in the shock layer. correlations do not work anymore.

# Validation of Aerothermodynamic Databases: Shock-Tubes Experiments

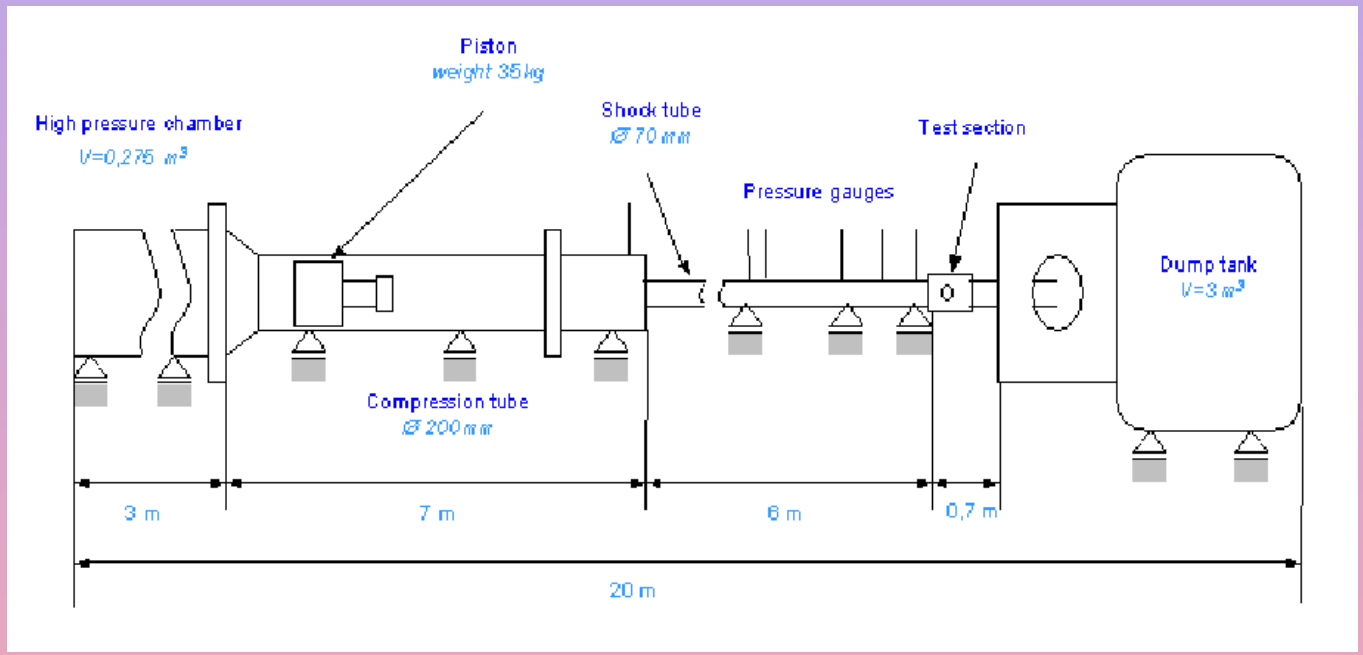


- TCM2 Shock-Tube at Marseilles, France, was utilized for validating the CFRD models used for Huygen's Entry

# Acquisition Results: CN spectral time-resolved picture

**Shot conditions :**

- Shock Tube
  Classical mixture
  $p_{shock}$=200 Pa
- Shock velocity
  $v_{shock}$=5680 m/s

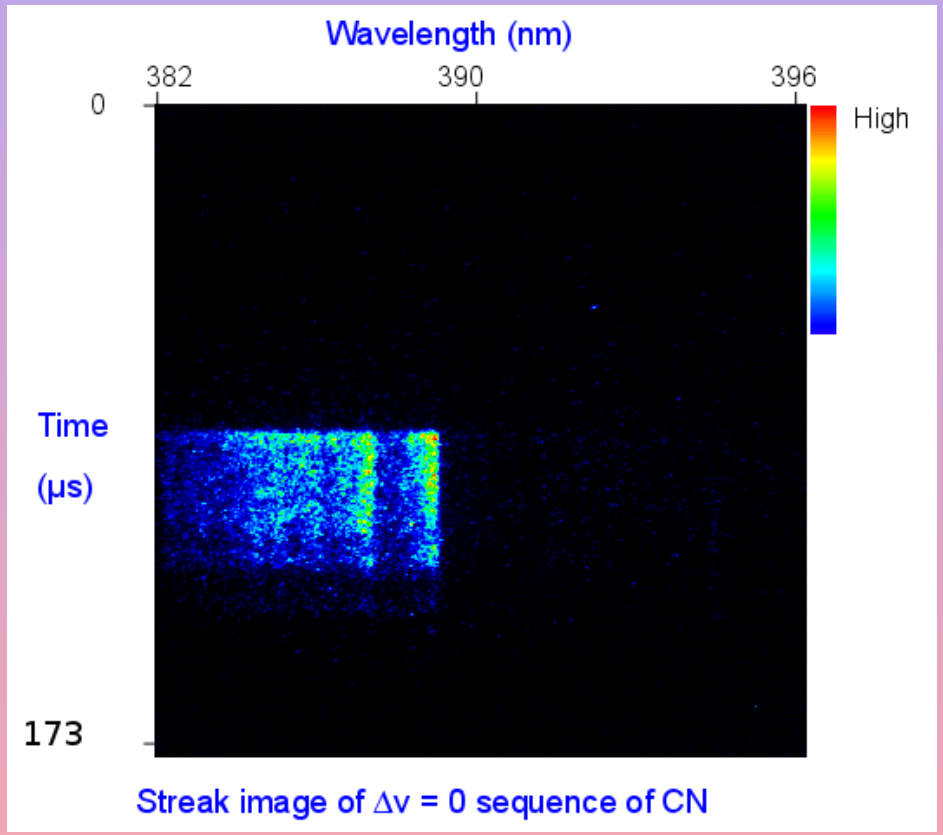

Streak image of Δv = 0 sequence of CN

# 40 Pa test rebuilding, Boltzmann

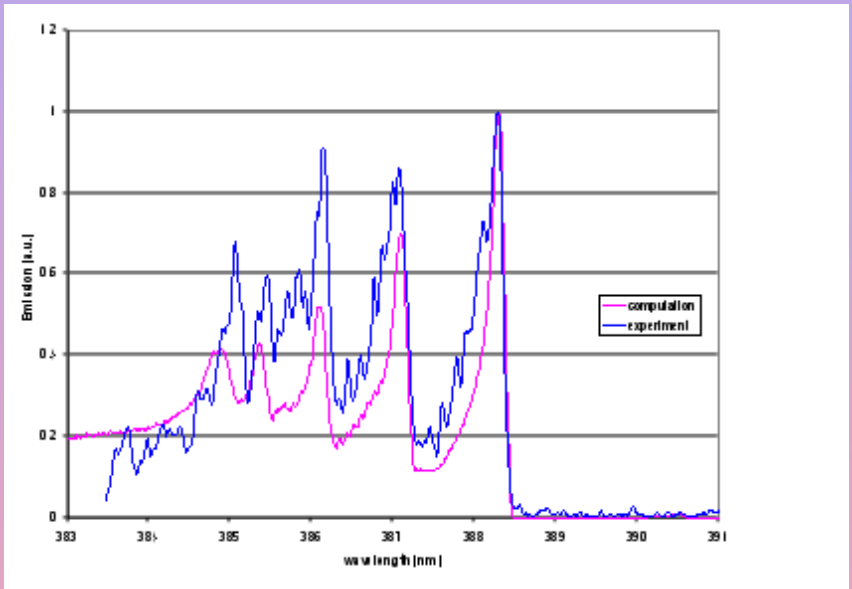


Non-equilibrium zone, 1s integration

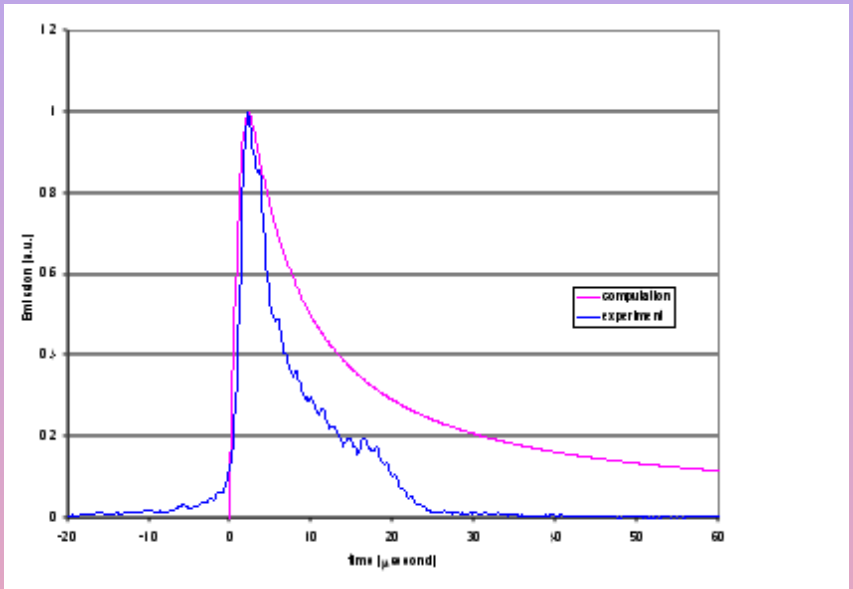


Temporal evolution

Validation of Aerothermal databases against simpler (1D, time-dependent) representative flow conditions

# Coupled CFD-Radiatve Simulations of Huygens Entry

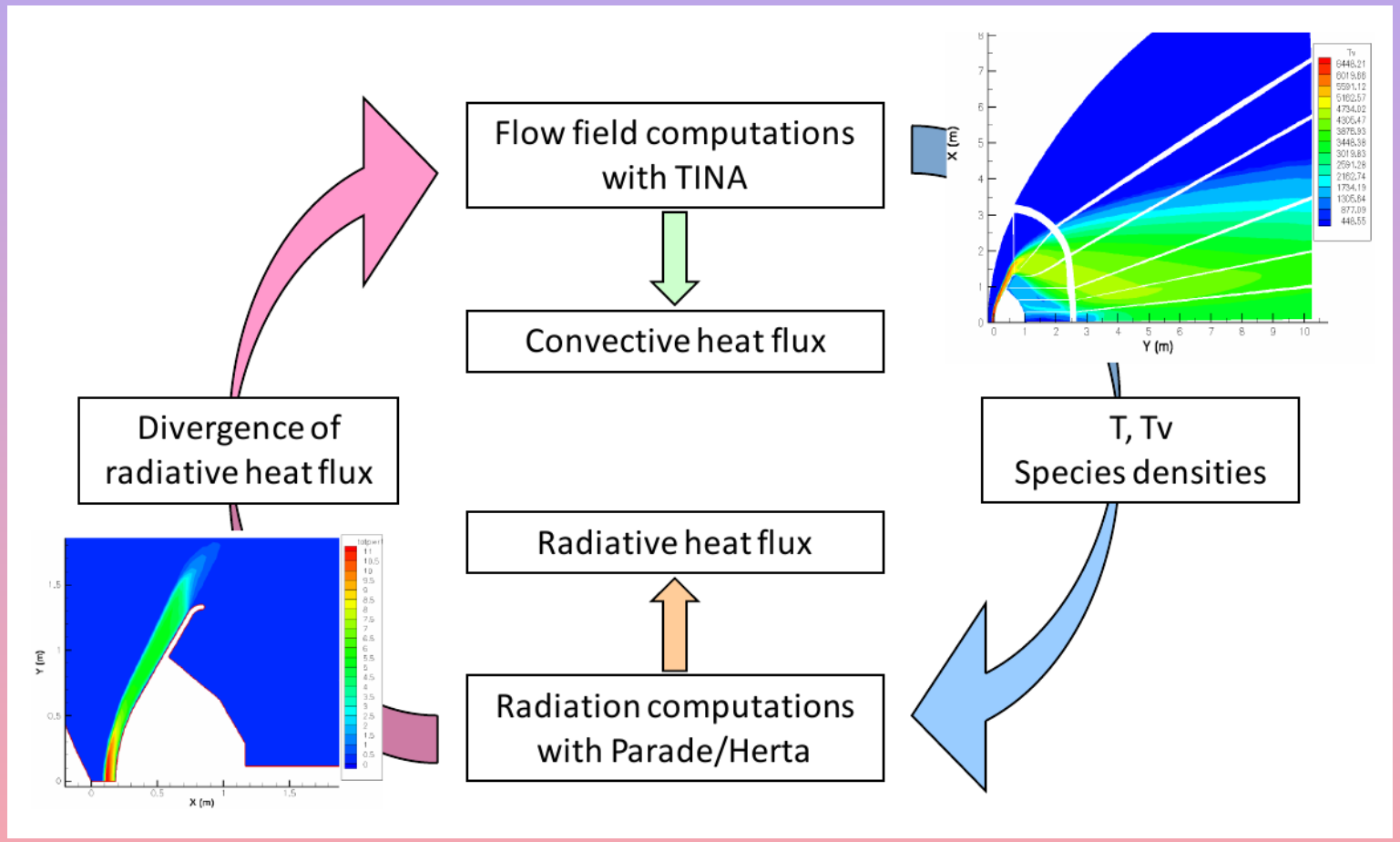

# Stagnation Streamline Temperatures Variation During CFD-Radiation Iterations

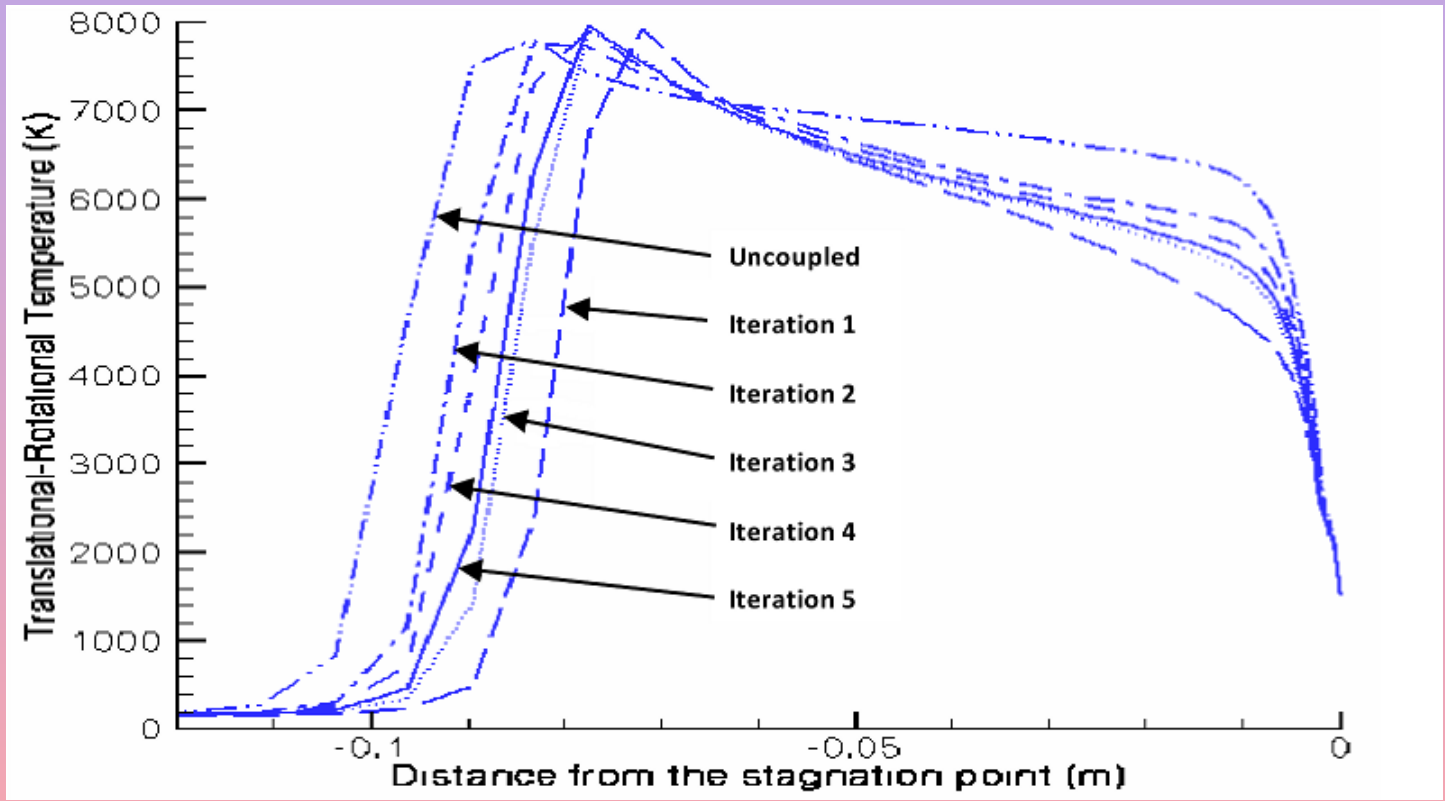

# Spectral Convergence

**Table 1: Influence of number of points for radiative heat flux**

| | | Without Absorption | | With Absorption | |
|---|---|---|---|---|---|
| Nb points | Resolution (pt/Å) | Q rad kW/m2 | Variation % | Q rad kW/m2 | Variation % |
| 5 000 | 0.28 | 2091.33 | +0.05 | 1773.38 | +30.58 |
| 50 000 | 2.78 | 2091.00 | +0.03 | 1603.38 | +18.06 |
| 100 000 | 5.56 | 2090.96 | +0.03 | 1535.54 | +13.07 |
| 200 000 | 11.1 | 2090.59 | +0.01 | 1488.07 | +9.57 |
| 1 800 000 | 100 | 2090.28 | - | 1358.08 | - |

# Influence of Radiation and Radiation Coupling

| Radiative heat flux | | Without coupling | With coupling |
|---|---|---|---|
| Without Absorption | kW/m2 | 813.82 | 516.82 |
| With Absorption | kW/m2 | 558.41 | 401.87 |

| Variation | | Without coupling | With coupling |
|---|---|---|---|
| Without Absorption | % | - | -36% |
| With Absorption | % | -31% | -51% |

# Phoebus High-Speed Entry Demonstrator

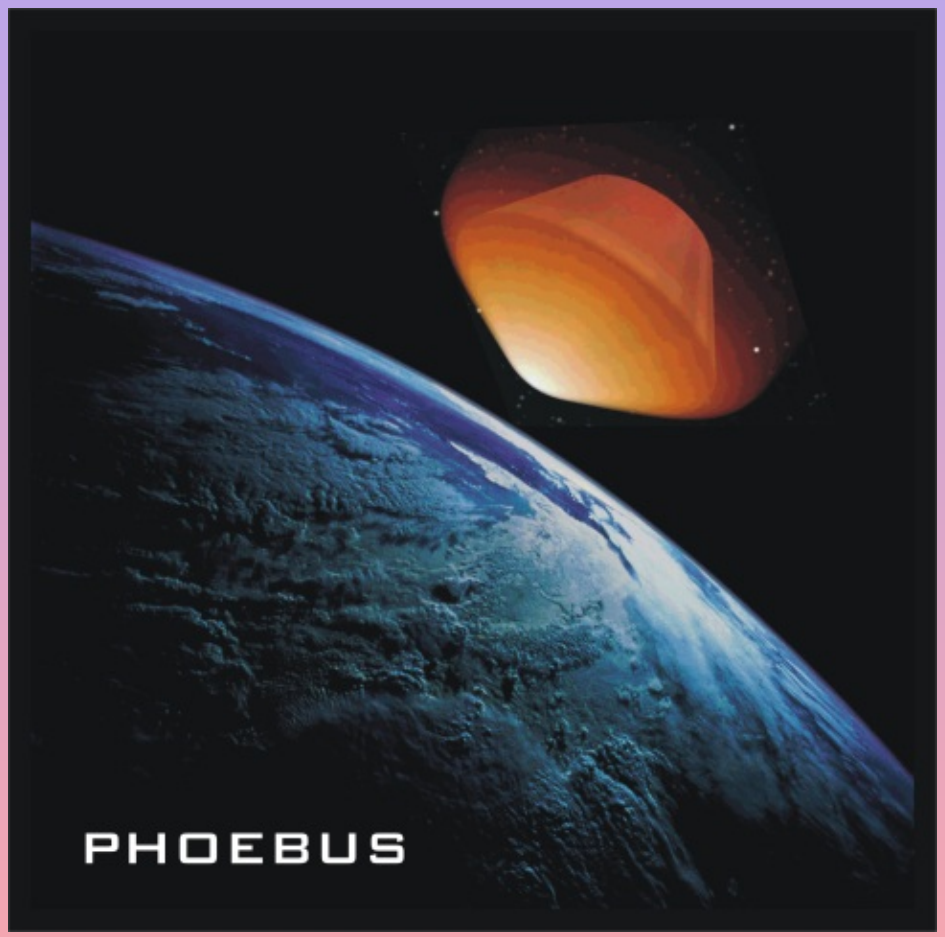


Table 9.2: *Phoebus simulation trajectory points and specifics of the corresponding freestream*

| Name | Time | Altitude | $\rho_\infty$ (kg/m$^3$) | $T_\infty$ (K) | $p_\infty$ (Pa) | $u_\infty$ (m/s) | Mach |
|---|---|---|---|---|---|---|---|
| TP1 | 18.4 | 64981 | 1.64e-4 | 233.3 | 10.96 | 10916 | 35.65 |
| TP2 | 21.8 | 55449 | 4.23e-4 | 254.0 | 30.96 | 10044 | 32.04 |
| TP3 | 24.1 | 49464 | 1.10e-3 | 270.6 | 85.28 | 9518 | 28.86 |
| TP4 | 26.0 | 45004 | 2.00e-3 | 264.2 | 149.10 | 8456 | 25.95 |

# Coupled Radiative Calculations with Ablation and Boltzmann Nonequilibrium Effects

## Stagnation point – Radiative heating

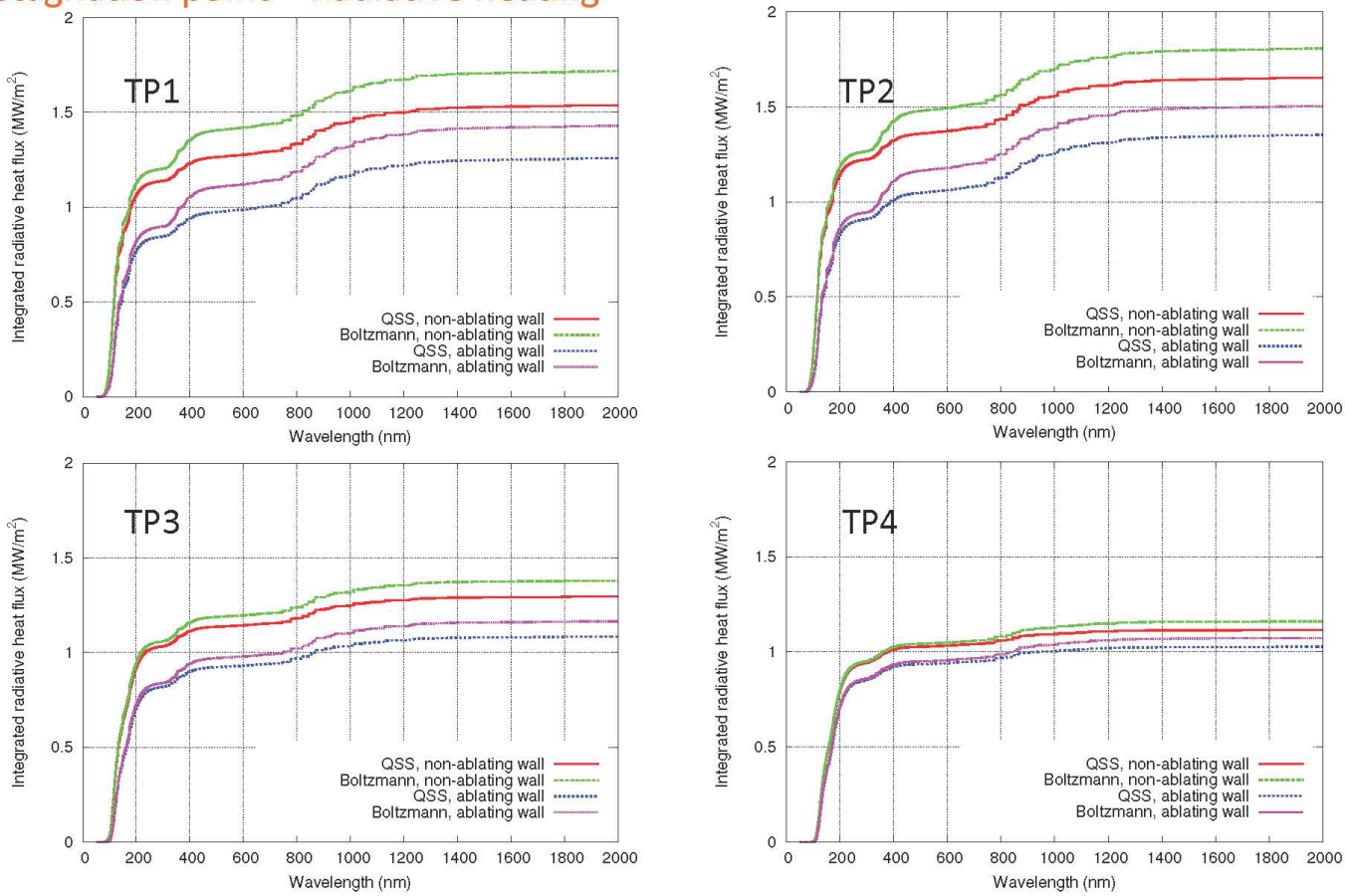


Courtesy O. Joshi (EPFL)

# Mars EXPRESS Observation of the PHOENIX Entry

- ESA Mars EXPRESS Orbiter provided support for PHOENIX 2008 Mars Entry
- Mars EXPRESS Tracked PHOENIX Entry with his onboard instrumentation (First Attempt at tracking an Entry from an Onboard Satellite).

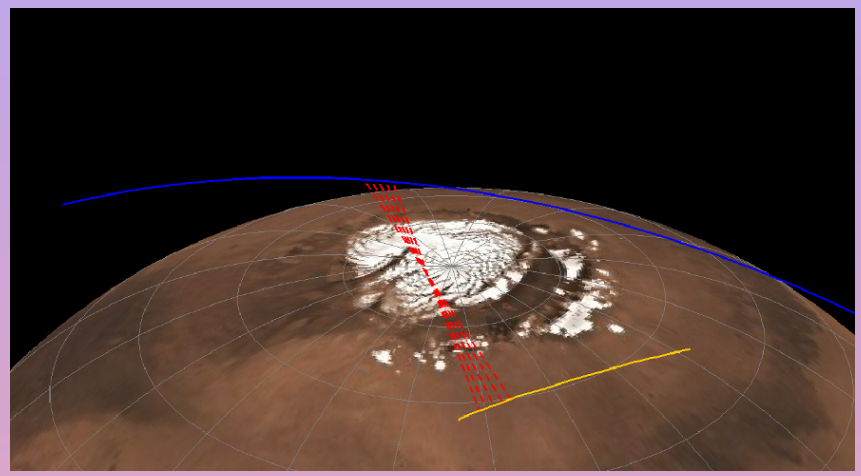

- CFRD simulations prior to entry predicted the IR trail to be the most emissive.
- SPICAM VUV Camera and HRSC Visible Camera tracked the Entry. IR Fourier Spectrometer could not be turned on due to power budget constraints.

# CFRD Simulations of PHOENIX Entry

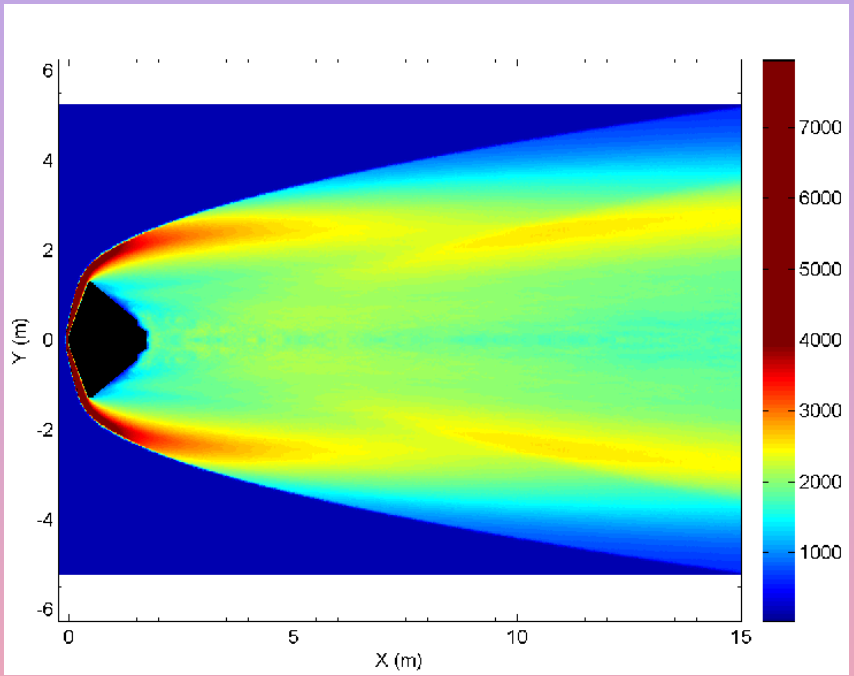


PHOENIX Temperature Profiles, t=203s

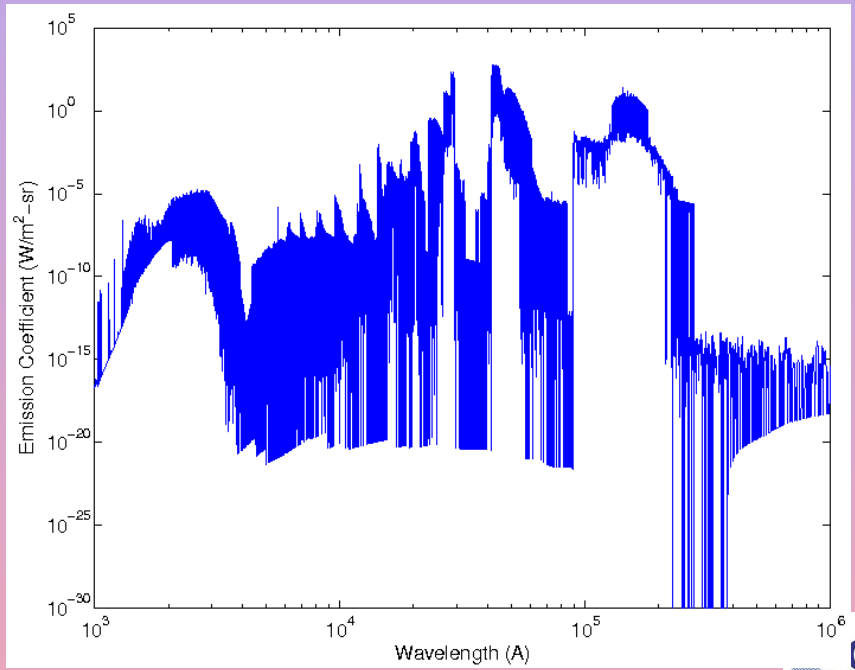


Sample spectrum of the PHOENIX Plume

# Radiative Transfer Towards Mars EXPRESS

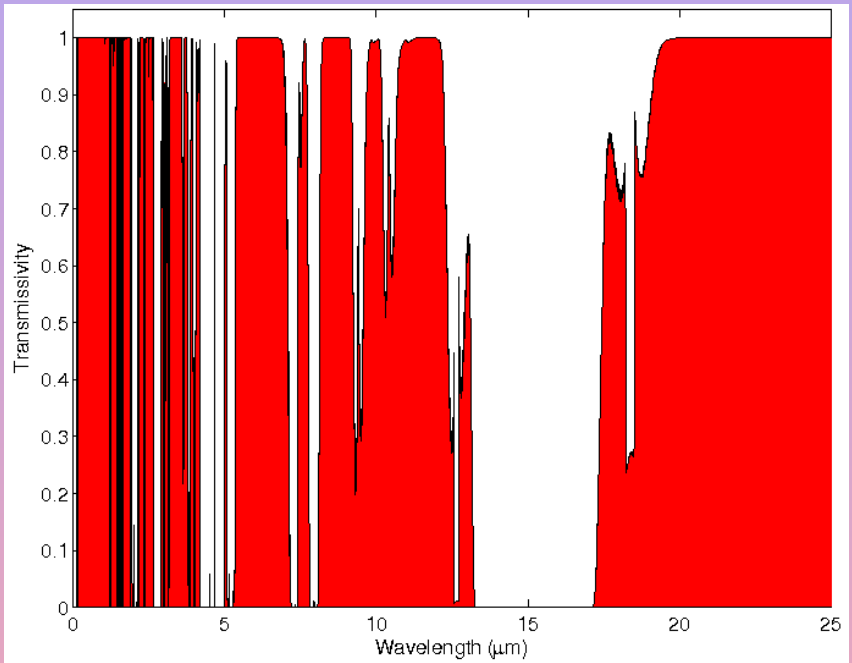


Optical path Transmissivity

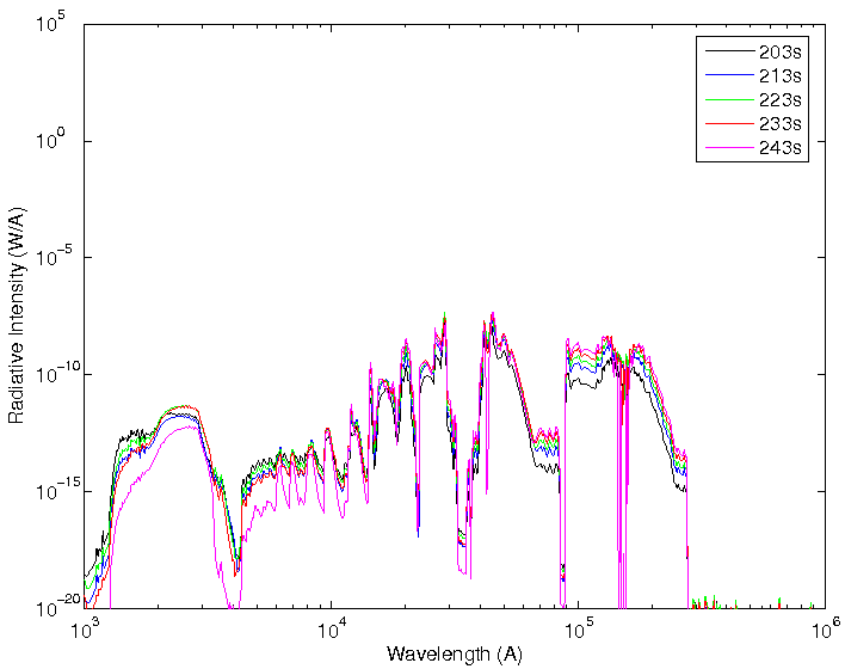


Raddiation collected by one pixel of the Mars EXPRESS instrumentation

Radiation in the VUV-Visible region was not detected, IR radiation was predicted to be detected if the instrument had been switched on

# Spectral Database for $CO_2$–$N_2$ Mixtures

- $CO_2$ Infrared
- CO Infrared
- CO $4^+$
- CO $3^+$
- CO Angstrom
- CO Triplet
- CN Violet
- CN Red
- $C_2$ Swan
- $C_2$ Phillips
- $C_2$ Mulliken
- $C_2$ Deslandres–D'Azambuja
- $C_2$ Ballik–Ramsay
- $O_2$ Sch.–Runge
- $O_2$ Sch.–Runge Cont.
- $N_2$ $1^+$
- $N_2$ $2^+$
- NO Gamma
- NO Beta
- NO Delta
- NO Epsilon
- NO Beta
- C Atomic
- C Photoionization
- N Atomic
- N Photoionization
- O Atomic
- O Photoionization
- $C^-$ Photodetachment
- $N^-$ Photodetachment
- $O^-$ Photodetachment
- $CO_2$ Photoionization
- $N_2$ Photoionization
- $O_2$ Photoionization
- CN Photoionization
- CO Photoionization
- NO Photoionization

# Radiative Power for $CO_2$–$N_2$ Mixtures: Comparison With Other Spectral Databases

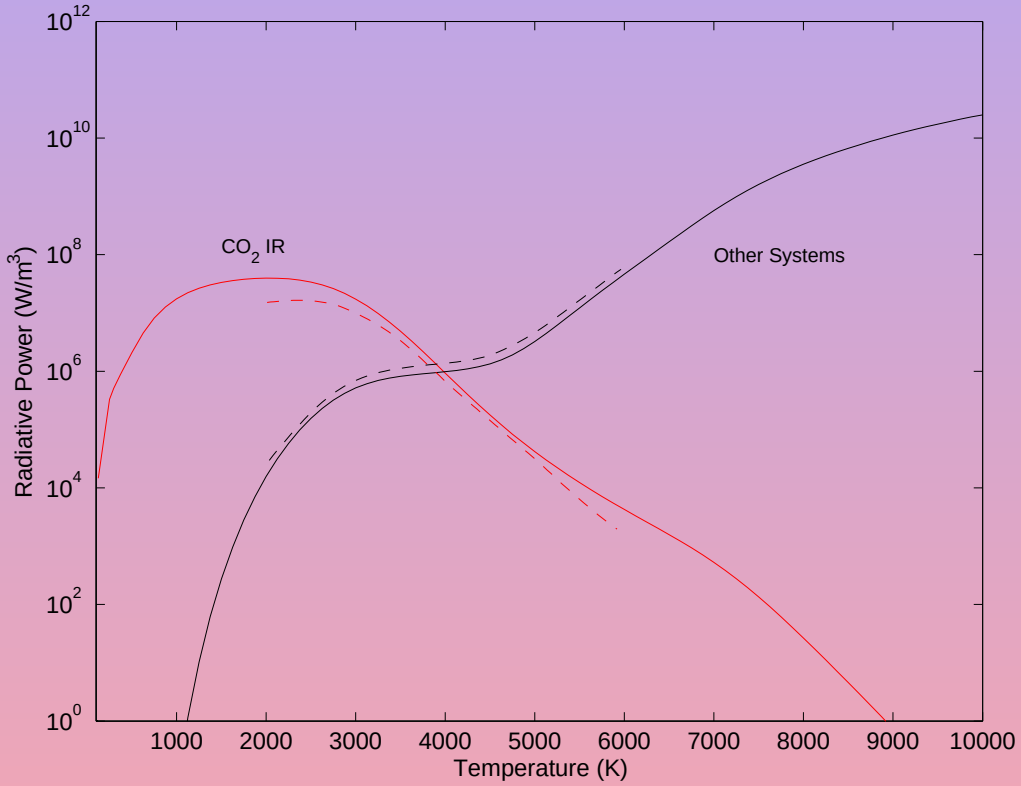


Comparison of the overall temperature dependent radiative power of $CO_2$ IR radiation (red) and for the other radiative systems (black) for an atmospheric pressure, Martian-type $CO_2$–$N_2$ plasma. Comparison is carried for the SPARTAN code database (full lines) and the EM2C database (dotted lines).

# Example of a Ray Departing from the Afterbody Plume; PH (1/2)

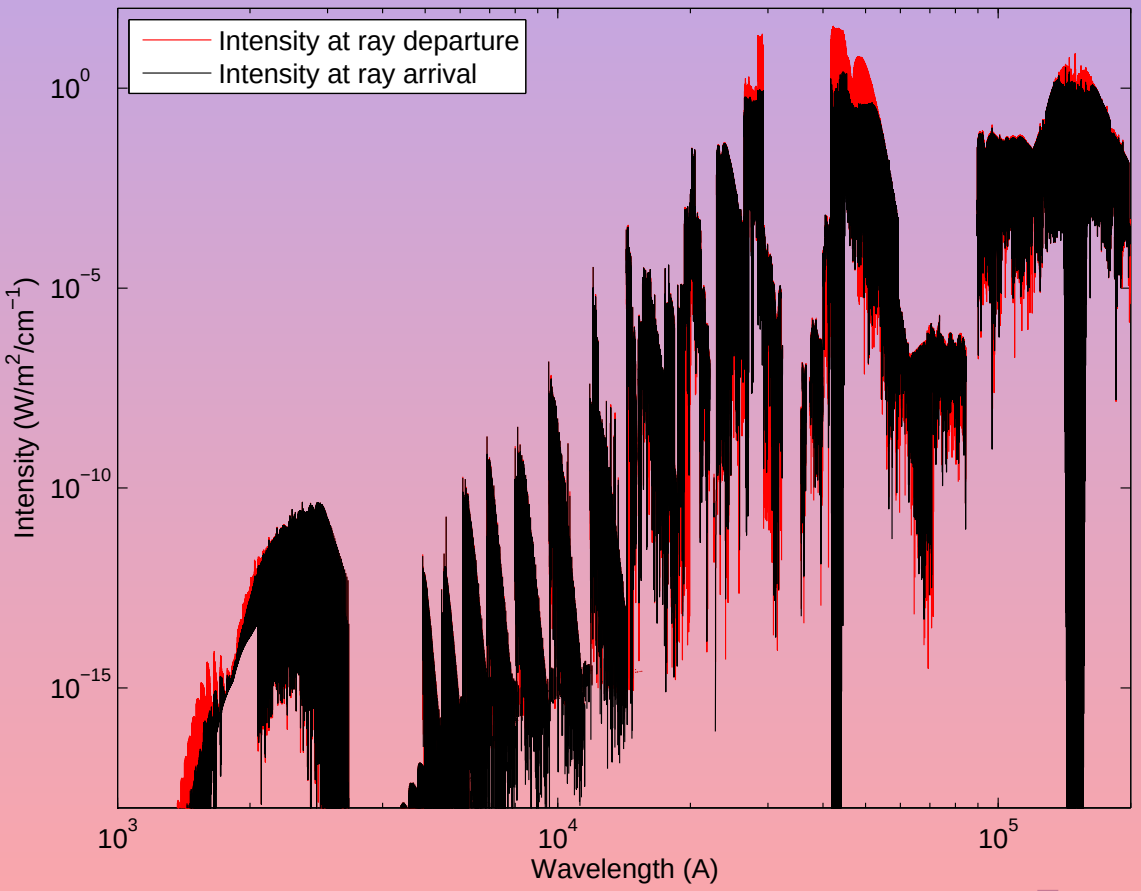

# Example of a Ray Departing from the Afterbody Plume; PH (2/2)

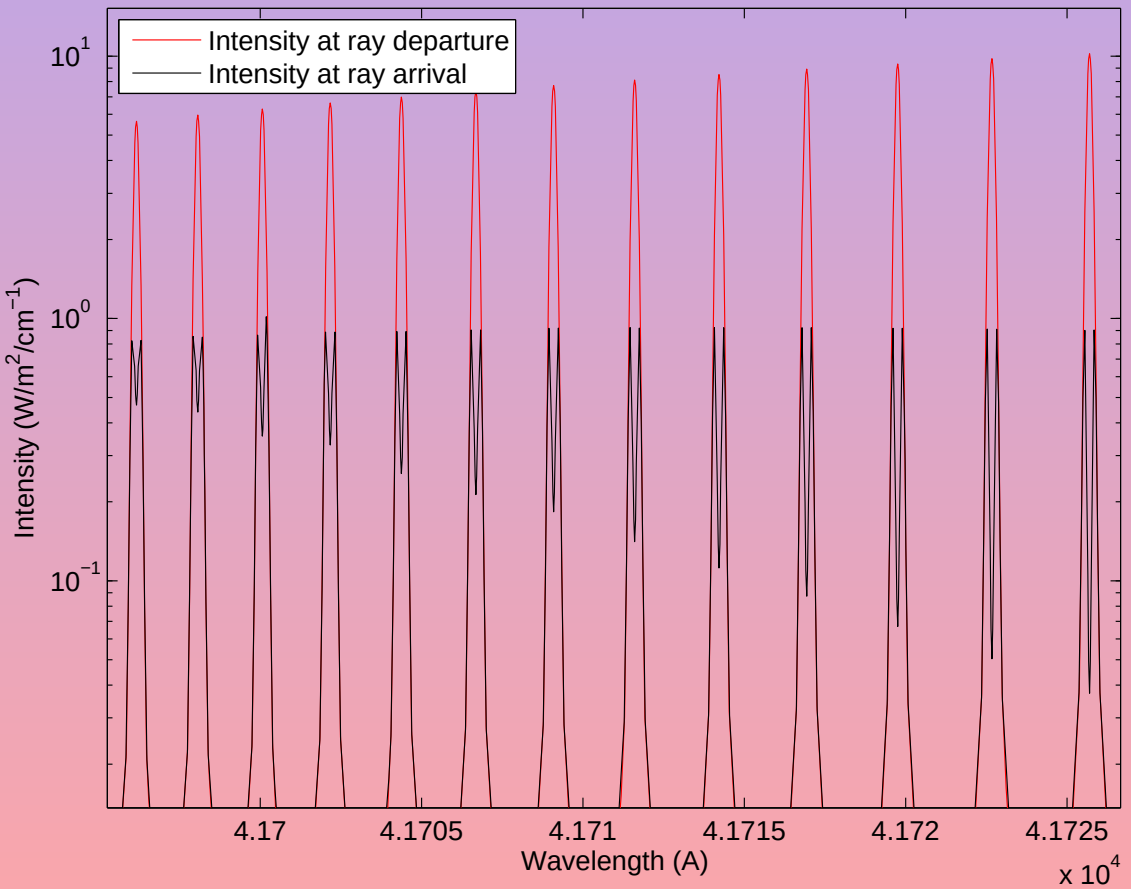

# Spectral Distribution of the Wall Fluxes; PH

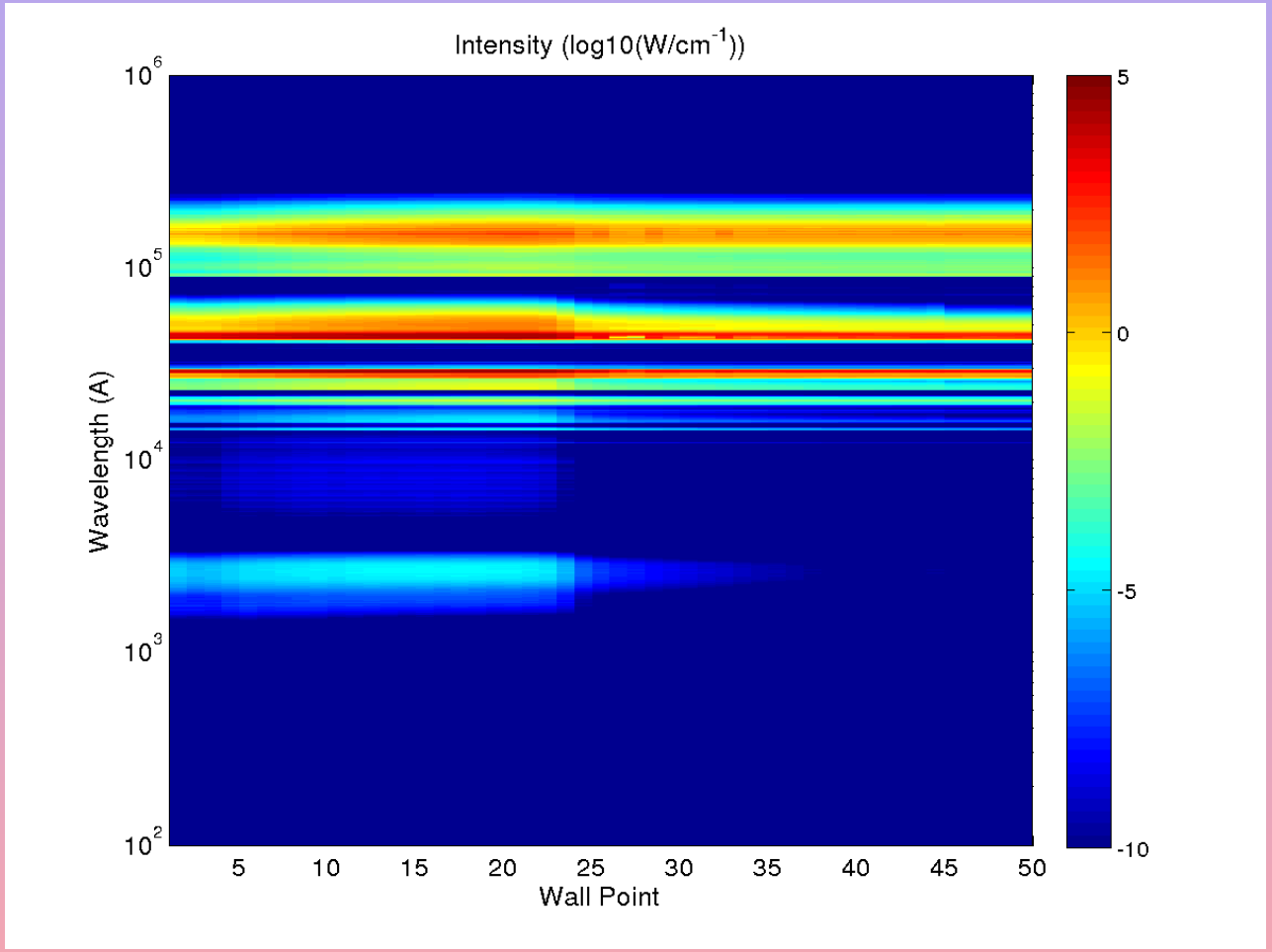


$CO_2$ IR radiation is dominant, with traces of CO $4^+$, CO $3^+$, and CO Angstrom in the forebody

# Comparison of Stagnation Streamline and Backcover Shoulder Spectra; PH

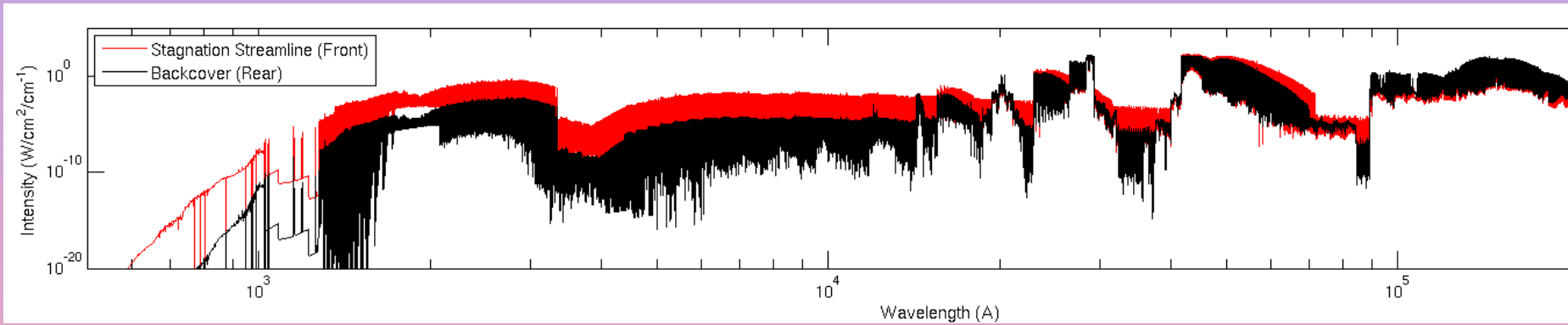


- VUV-Visible radiation higher for the stagnation streamline points
- For both points, $CO_2$ radiation spectral intensity is several orders of magnitude above Visible-VUV radiation

# Contribution of Radiative Fluxes above 1$\mu$m to the Overall Radiative Power; Large Spacecraft Configuration

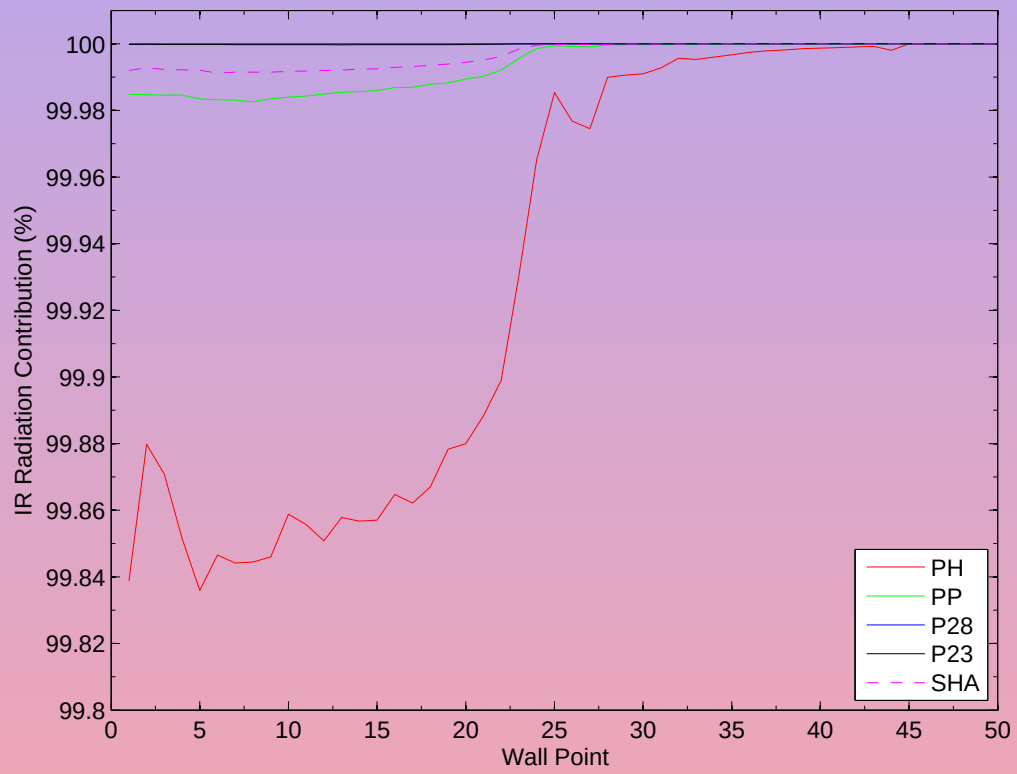


Values for the smaller spacecraft configuration are similar. Other studies in the scope of the ESA TC3 testcase confirm such findings for $CO_2$–$N_2$ mixtures (CN and $C_2$ radiation less than 3% overall in the stagnation streamline point.

# Sensitivity Studies

- Ray-tracing calculations carried for peak conductive heating (PH; Tv/T 1.2) either considering (T,Tv) or just (T).
- Ray-tracing calculations carried at 2.8km/s (P28) with a 5m and a 7.5m afterbody flow.
- Influence of thermal nonequilibrium less than 5% on wall fluxes, and enough backflow is accounted for (3% diff. max).

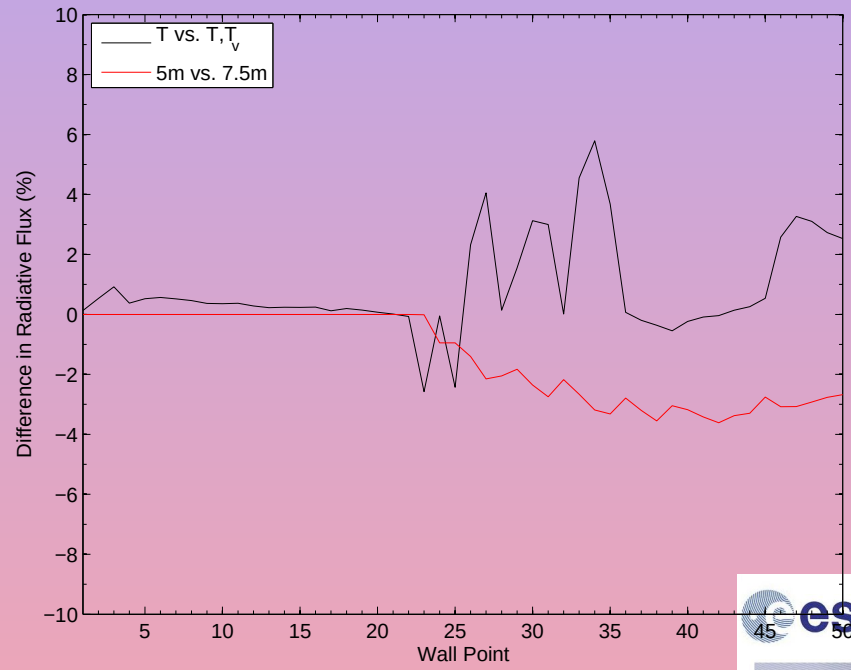

# A Careful Tailoring of Spectroscopic Databases Allows Very Good Fits of Equilibrium Radiation

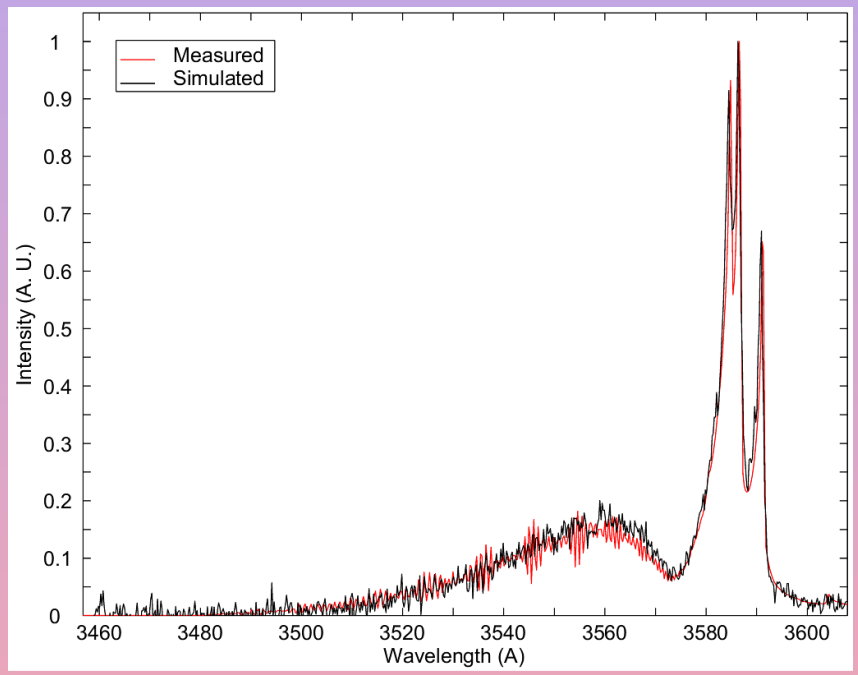


Best-fit to a measured CN Violet Spectrum ($\Delta v = 1$)

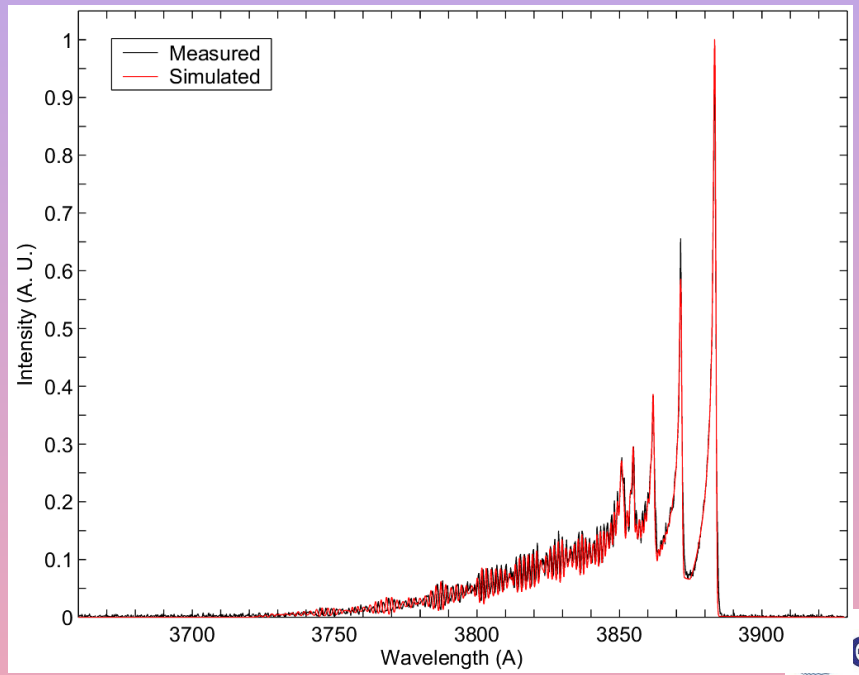


Best-fit to a measured CN Violet Spectrum ($\Delta v = 0$)

esa

INSTITUTO SUPERIOR TÉCNICO

Spectra measured in equilibrium conditions in an ICP torch (97% $CO_2$–3% $N_2$ gas)

# But Radiation is not Always Boltzmann!

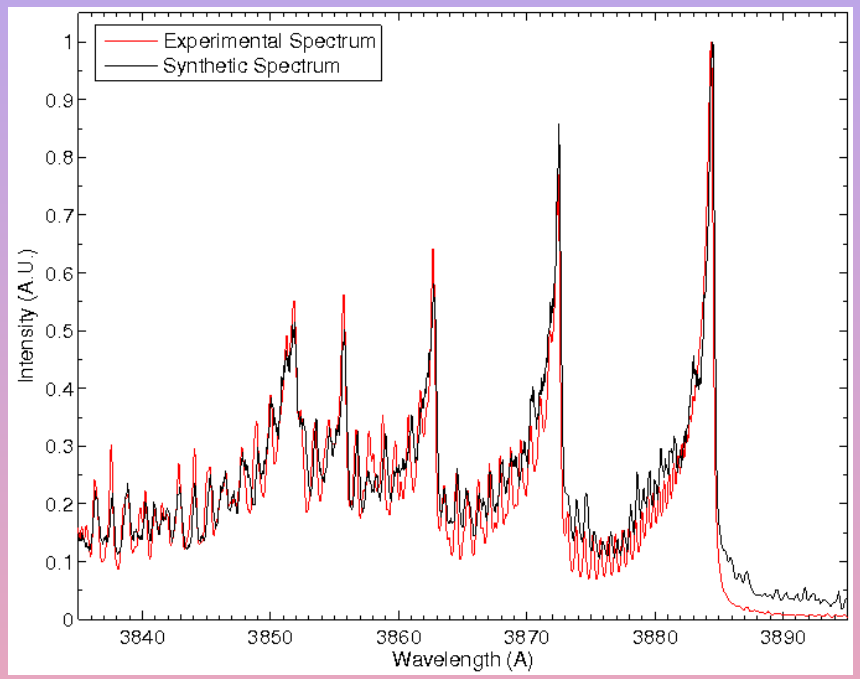


Fitting of the CN Violet system, assuming $T_r$=10000K and a Boltzmann vibrational distribution

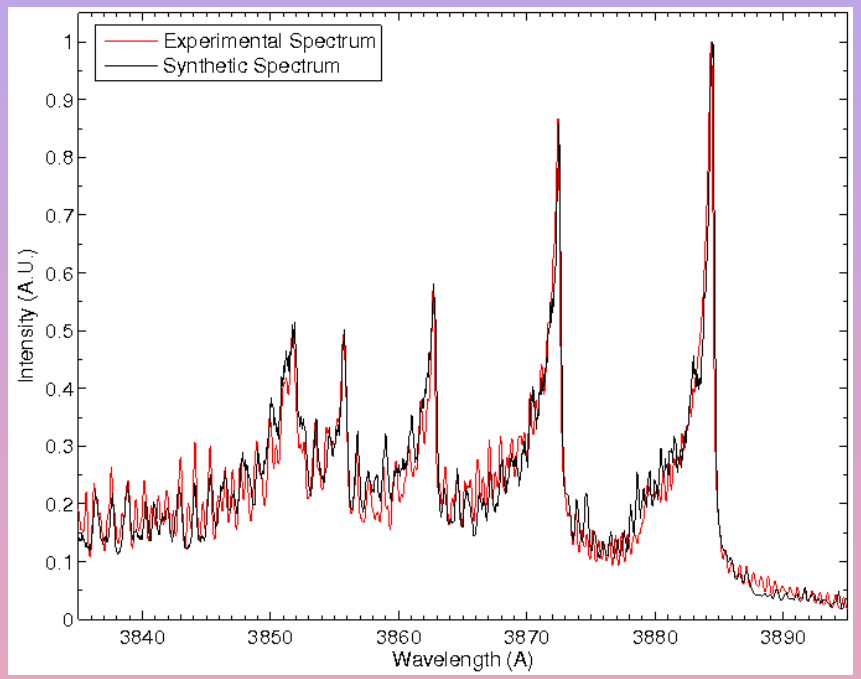


Fitting of the CN Violet system, assuming $T_r$=2700K and a non-Boltzmann vibrational distribution

Fitting of a strongly nonequilibrium CN Violet Spectra obtained in a Supersonic Arc-Jet for a Titan-type (95% $N_2$–5% $CH_4$ gas)

# But Radiation is not Always Boltzmann!

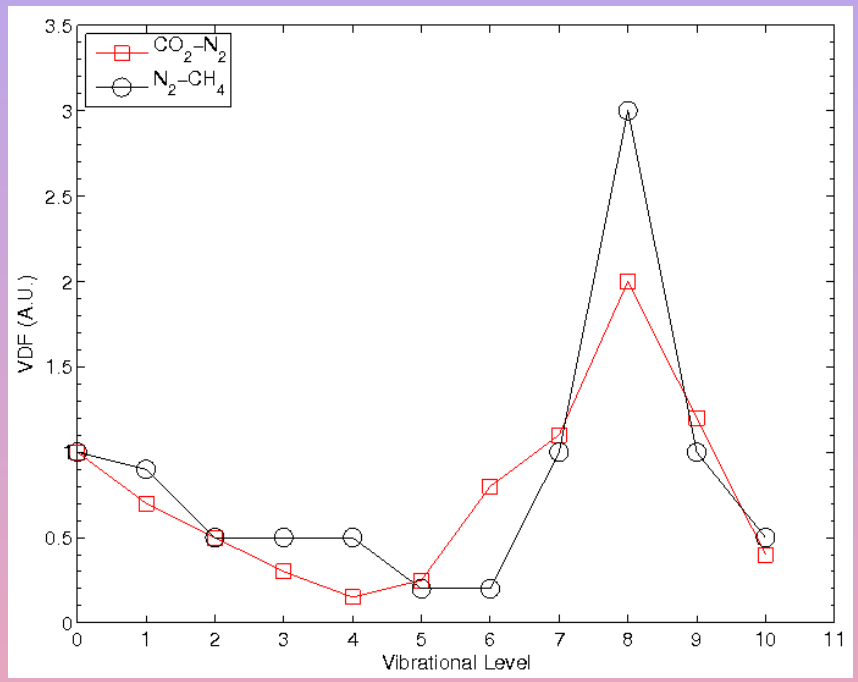


non-Boltzmann vibrational distribution Function

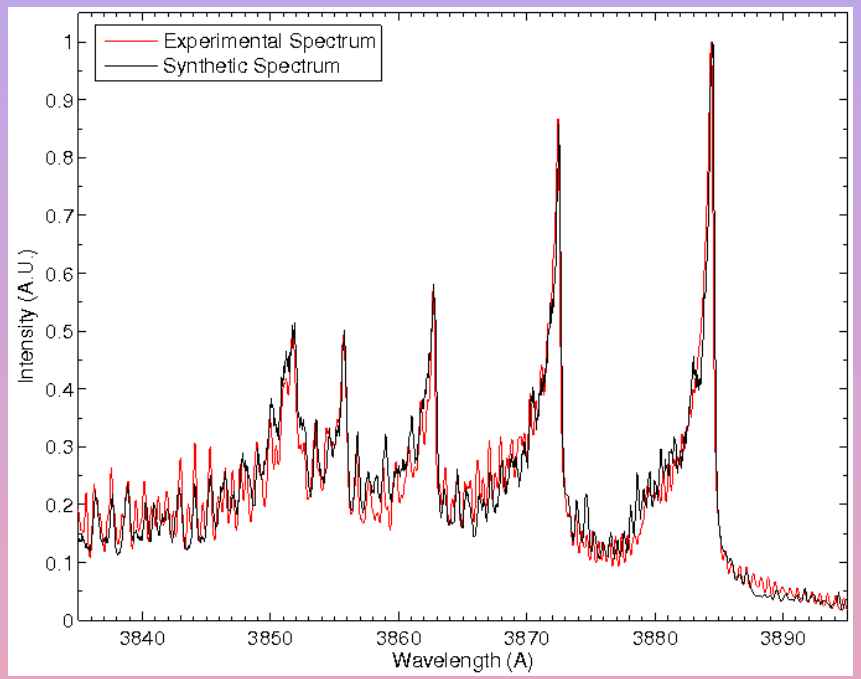


Fitting of the CN Violet system, assuming $T_r$=2700K and a non-Boltzmann vibrational distribution

Fitting of a strongly nonequilibrium CN Violet Spectra obtained in a Supersonic Arc-Jet for a Titan-type (95% $N_2$–5% $CH_4$ gas)